Early effects of perinatal hypoxia and resuscitation on cerebral perfusion and metabolism assessed by MRI, CEUS and FDG-PET. Experimental studies in newborn pigs.

Charlotte de Lange

PhD thesis

Faculty of Medicine, University of Oslo

2012

Department of Paediatric Research

and

Department of Radiology and Nuclear Medicine

Oslo University Hospital

Rikshospitalet

Norway

Series of dissertations submitted to the
Faculty of Medicine, University of Oslo
No. 1429

ISBN 978-82-8264-477-8

Cover: Inger Sandved Anfinsen.
Printed in Norway: AIT Oslo AS.

Produced in co-operation with Akademika publishing.
The thesis is produced by Akademika publishing merely in connection with the thesis defence. Kindly direct all inquiries regarding the thesis to the copyright holder or the unit which grants the doctorate.

Contents

1. Abstract of thesis

Birth asphyxia is worldwide, still an important cause of child morbidity and mortality. Early detection of cerebral hypoxic ischemic (HI) injury is important in order to start neuroprotective treatment. Neuroimaging methods play an important role in the diagnosis and prognosis, and magnetic resonance imaging (MRI) is considered the most specific and sensitive method. However, MRI is expensive and difficult to perform during the short therapeutic time window after the insult. In asphyctic newborn infants, resuscitation with high-level oxygen ventilation has proven harmful to the organs and consequently resuscitation with air is now recommended.

This thesis introduces and evaluates radiological and nuclear medicine methods for use in newborn piglets, to detect early effects and mechanisms of perinatal cerebral HI and resuscitation related to injury. Using a piglet model, cerebral perfusion, diffusion and glucose metabolism were studied. Changes during and after hypoxia/hypoxia-ischemia were correlated to the resuscitation mode and histopathologic findings.

In 3 different studies, contrast enhanced ultrasonography (CEUS) and dynamic susceptibility contrast (DSC) enhanced-, diffusion weighted- (DWI) MR imaging, MR spectroscopy (MRS) and Positron emission tomography with fluorodeoxyglucose (FDG-PET), were used.

Our findings confirmed that HI injury in the piglet could reveal diffusion and MRS changes correlated to injury, and this is in accordance with other clinical studies. After global hypoxia, CEUS revealed changes in cerebral perfusion, with decreased values during resuscitation with 100% O_2, not found when using air. The changes in MRI /CEUS perfusion were transient, with poor correlation to diffusion and histopathologic findings. Dynamic FDG-PET detected an immediate decrease of cerebral glucose metabolism after perinatal hypoxia. This may indicate early changes of mild cerebral HI injury. No significant influence of resuscitation with 100% O_2 versus air was found.

We conclude that the piglet model is suitable for assessing early changes of cerebral diffusion, metabolism and microvascular perfusion after HI injury. MRI, CEUS or FDG-PET cannot be used alone in the early detection of cerebral HI injury. These adapted techniques can provide further insights into the mechanisms of perinatal hypoxia-ischemia, where early detection plays an important role for instituting therapy.

2. Acknowledgements

The thesis was initiated and carried out at the Dept.of Paediatric Research, Oslo University Hospital, Rikshospitalet from 2008 to 2012 in collaboration with the Institute of Surgical Research, the Interventional Centre and the Centre for Molecular Biology and Neuroscience, Dept. of Anatomy, Institute of Basic Medical Sciences, University of Oslo. It was in part financially supported by grants from the Child foundation and Medinova foundation at Oslo University Hospital and the Norwegian SIDS and Stillbirth Society.

Experimental animal studies are very complex, necessarily involving many collaborators. This work is the result of the contribution from many skilled persons and scientists I had the privilege to collaborate with and that I would like to express my sincere gratitude to;

My principal supervisor Berit H Munkeby, MD, PhD. You are an enthusiastic person and inspired me to begin, go through, and finally complete this work. I am deeply grateful to you for introducing me to experimental research in piglets and perinatal hypoxic ischemic injury. These studies could not have been carried out without your help, knowledge about the piglet model and skills as anesthesiologist. I thank you for your optimism,inspiration and encouragement throughout this work.

I am deeply grateful to my co-supervisor Professor Ola Didrik Saugstad for giving me the opportunity to work within the field of perinatal hypoxic ischemic injury and resuscitation and for letting me perform radiological and nuclear medicine studies on the piglet model developed at your department. I would like to thank you for your encouragement, ideas and valuable scientific advice in completing this work

My co-authors at the Dept. of Radiology; Knut Brabrand, MD without your help, enthusiasm, inspiration and knowledge of contrast enhanced ultrasonography, this work would not have been possible. I am also very grateful to, John Hald, MD, PhD for your valuable help and neuroradiological advice.

I would like to express my special appreciation and thank you to my physicist co-authors contributing to this work, for their scientific knowledge, spirit, and answers to all my questions - always with a sense of humor. Professor Atle Bjørnerud and Kyrre Eeg Emblem, PhD. Your knowledge and skills in MR perfusion and statistics have been invaluable for this work. Professor Eirik Malinen, contributing with your invaluable knowledge and expertise in PET physics and chief engineer Hong Qu at the department of Anatomy for your important and valuable help during the performance of the study.

I am very grateful to Professor Else Marit Løberg, for your contribution with the histopathology. Professor Arne Skretting, and Kjersti Johnsrud, MD for their expertise, help and advice during the planning and performance of the FDG-PET study. Eirik Stokke MD,PhD for his help during the performance of one the studies.

Colleagues, collaborators and friends at the department of Paediatric Research, especially

Jannicke Andresen, MD, PhD and Grete B Kro, MD for their support, encouragement and contribution to first MRI study and to Rønnaug Solberg, MD, PhD for your nice support and fruitful discussions about the piglet model. I would also like to thank chief administrative officier Elisabeth Mathiassen for your kind assistance.

I would like to sincerely thank Professor Ansgar Aasen , head of Institute of Surgical Research, Professor Håvard Attramadal, and their staff for providing me excellent help and expertise during the animal experiments; Roger Ødegaard, Vivi Bull Stubberud, Sera T Sebastian, Aurora M Pamplona. At the Dept. of Comparative Medicine, I would like to thank the late chief veterinarian Dag Sørensen and especially engineer Kjersti Janette Kjos Wamstad, as well as the farmer, for their assistance and delivery of the piglets.

I am also very grateful for the invaluable help and expertise during performance of the experiments by many radiographers, bioengineers, nurses, physists at the Dept. of Radiology and Nuclear Medicine and the Interventional Centre. I thank especially, Eldrid Winther Larsen, Terje Tillung, Hilde Sofie Korslund, June-Cathrine Berge, Karl Øyri, Carmen Louwerens, Kersti Wendt, Frederic Courivaud, Oliver Geier, Ann-Eli Spiten and Ellen Gunnerud Kristoffersen for your contribution.

I would like to express my gratitude to my chief and head of the of Pediatric Radiology unit, Bjarne Smevik,, MD for your support and assistance in the performance of my thesis. I also thank the head of the section of Neuroradiology, Musculoskeletal- and Pediatric Radiology, Paulina Due-Tønnesen, MD and the head of the department Radiology and Nuclear Medicine, Professor Hans Jørgen Smith for their sincere support in this thesis.

Special thanks go to dear friends and colleagues at the department of Pediatric Radiology and Radiology for their encouragement and moral support throughout this work.

We are also very grateful to Siemens, Norway for your valuable contribution providing us with an ultrasound machine during the performance of one study and Bracco, Milan, Italy for providing of the ultrasound contrast agent. The Norwegian Medical Cyclotron Centre provided the radioactive tracer to the PET study, for which we are sincerely grateful.

My parents, Ulli and Per, thank you for your never-failing loving support and trust in me. Your long scientific experience has provided me valuable scientific advice and lots of encouragement during this work.
I would also like to especially thank my closest family Katarina, Jørg, Emil , Niklas and Harald, Margareth Jannicke and Cathrine also including all our dear friends, for your presence, support and important distraction (keeping me from working to much).

My lovely grown up sons, Christian and Jonas for your warm love, support and encouragement.

Finally, my special love and outmost thank you to my husband Thomas, for your support and patience. Your continuous encouragement and enthusiasm have been invaluable and truly necessary for this work to be completed.

3. List of publications

This thesis is based on the following papers, which will be referred to by their Roman numerals:

I. Munkeby BH, de Lange C, Emblem KE, Bjørnerud A, Kro GA, Andresen J, Winther-Larssen EH, Løberg EM, Hald JK.
A piglet model for detection of hypoxic-ischemic brain injury with magnetic resonance imaging, Acta Radiol. 2008 Nov;49(9):1049-57

II. de Lange C, Brabrand K, Emblem KE, Bjørnerud A, Løberg EM, Saugstad OD, Munkeby BH.
Cerebral perfusion in perinatal hypoxia and resuscitation assessed by trans cranial contrast enhanced ultrasound and 3T MRI in newborn pigs.
Invest Radiol. 2011 Nov;46(11):686-96

III. de Lange C, Malinen E, Qu H, Johnsrud K, Skretting A, Saugstad OD, Munkeby BH.
Dynamic FDG-PET for assessing early effects of cerebral hypoxia and resuscitation in newborn pigs. Eur J Nucl Med. 2012 Feb 2, Epub ahead of print.

4. Selected abbreviations

ADC Apparent diffusion coefficient

ASL Arterial spin labeling

ATP Adenosine triphosphate

AUC area under the curve

BG basal ganglia

CA contrast agent

CBV cerebral blood volume

CBF cerebral blood flow

CMR_{gl} Cerebral metabolic rate of glucose

CEUS contrast enhanced ultrasonography

DSC-MRI dynamic susceptibility contrast enhanced MRI

DWI diffusion weighted imaging

DTI diffusion tensor imaging

EEG Electroencephalogram

FA fractional anisotropy

FDG-PET (^{18}F) 2-deoxy-2-fluoro-D-glucose-positron emission tomography

FiO_2 fraction of inspired oxygen

^{1}H MRS proton MR spectroscopy

HI hypoxic ischemic

HIE hypoxic ischemic encephalopathy

HR heart rate

LC lumped constant

MABP mean arterial blood pressure

MRS MR spectroscopy

MTT mean transit time

PI peak intensity

PWI perfusion weighted imaging

ROI region of interest

SNR signal to noise ratio

SUV standardized uptake value

TTP time to peak

US ultrasonography

5. Introduction

5.1 Perinatal hypoxic ischemic (HI) injury

5.1.1 Definition

Birth asphyxia is still one of the major causes of chronic handicaps and death in children worldwide and is highest in developing countries (1;2). Of 140 million annual births worldwide 4-9 million suffer from birth asphyxia (3). Despite improvements in neonatal practice the incidence of deaths of about one million has remained essentially unchanged while one million develop severe organ injury, resulting in a burden of 42 million disability adjusted life years (4;5). The financial, medical and social burdens of birth asphyxia are poorly quantified, but undoubtedly substantial.

Birth asphyxia is defined as a condition with impaired gas exchange leading to hypoxemia, hypercapnia and metabolic acidosis. All of the following criteria must be fulfilled in order to define an asphyctic condition (6).

- Evidence of metabolic acidosis in fetal umbilical cord arterial blood at delivery (ph<7 and base deficit ≥12 mmol/L).
- Apgar score of 0-3 for five minutes or more.
- Evidence of neurological disturbance (e.g. seizures, coma, hypotonia) and one or more of the following organ system injuries; cardiovascular, gastrointestinal, hematological, pulmonary, renal, or hepatic dysfunction.

Birth asphyxia may result in hypoxic ischemic encephalopathy (HIE) in term or late preterm infants. It is a clinically defined syndrome of disturbed neurological function in the earliest days of life manifested by difficulty with initiating and maintaining respiration, depression of tone and reflexes, subnormal level of consciousness and often by seizures (7).

5.1.2 HI injury mechanisms

HIE follows upon a disruption of cerebral blood flow (CBF) and oxygen delivery to the brain most likely caused by reduced placental blood flow and gas exchange before, during, or after birth. Several factors such as timing, duration and severity of the insult and the maturity of the brain influence the development and degree of injury. Severe acute HI injury rapidly results in neuronal death while less severe but prolonged insult leads to greater injury by apoptosis (activation of genetically determined cell-death programs) (8).

Clinical and experimental observations demonstrate that HI injury is not a single "event" but rather an evolving process (8;9). Brain injury is thought to occur in 2 phases separated by a brief recovery or latent phase (10). During the **acute phase or "primary energy failure"** CBF decreases due to interrupted placental blood flow and delivery of oxygen to the brain, leading to acidosis. This acute reduction of CBF and oxygen delivery initiates a cascade of deleterious biochemical events. Depletion of oxygen causes switch to anaerobic metabolism (dominated by anaerobic glycolysis) resulting in 1.a rapid depletion of high-energy phosphate reserves including adenosine triphosphate (ATP), 2. accumulation of lactic acid, and 3. inability to maintain cellular functions. This loss of cell membrane integrity and function causes a loss of electrolyte ionic gradients. Intracellular sodium, calcium and water shift cause cell swelling and necrosis. In parallel, potassium leaks into the extracellular space inducing a slow depolarization and release of neurotoxic excitatory neurotransmitters, in particular glutamate. Glutamate then causes an influx of calcium and sodium into postsynaptic neurons causing a rapid depolarization. In addition, free fatty acids accumulate and undergo peroxidation by free oxygen radicals that arise from reductive processes with byproducts of prostaglandins, xanthine and uric acid. Intracellular calcium may induce a production of the free radical nitric oxide (NO) that diffuses to adjacent cells susceptible to NO toxicity. The combined effect of cellular energy failure, acidosis, glutamate release, intracellular calcium accumulation, lipid peroxidation and NO neurotoxicity destroy essential components of the cell, resulting in cell death. The duration or severity of the insult commands the progression and severity of injury. If oxygen is restored by reoxygenation, brain oxidative metabolism and cellular pH recover briefly during the **"latent period"** which does not seem to extend for longer than 6 h (4;8;11).

The **delayed phase or "secondary energy failure"** appears and evolves 6 to about 48 h after the hypoxia-ischemia. During this phase, intracellular pH and phosphorus metabolites return to baseline and cardiorespiratory status is stable, contributing to further brain injury (8;10). The injury mechanisms during the secondary phase include iron accumulation, mitochondrial failure and injury from inflammatory mediators that initiate apoptosis. The role of inflammation in HI brain injury is complex but seems to give both some beneficial and deleterious effects after injury.

It is during the transition from the recovery (latent) phase to the secondary phase that there is a potential for diminution of injury by neuroprotective intervention (8;12).

Cerebral perfusion in HI injury

Perfusion or blood flow is a biological process that assures a sufficient supply of cell nourishment, removal of metabolic waste and maintenance of body temperature. Cerebral perfusion mirrors cerebral metabolic demand and neuronal function, and therefore, is a vital parameter in the evaluation of HI brain injury and recovery. CBF has regional differences with the highest perfusion in basal ganglia /thalamus region in term babies. During the brain maturation, cerebral vasculature develops in different regions at different time points influencing the pattern of injury.

The effect of hypoxia-ischemia on cerebral perfusion has been experimentally studied (fig.1) (13). Laboratory studies suggest that most hypoxic injuries in fetuses and infants reflect combinations of hypoxia and ischemia rather than hypoxia alone. Decrease in cerebral perfusion is necessary for the development of brain injury by a combination of oxygen deficit and superimposed ischemia or isolated ischemia (14;15).

During hypoxia, there is an activation of the sympathetic adrenergic system redistributing the cardiac output in favor of the central organs. The decreased oxygen and increased carbon dioxide partial pressures lead to a vasodilation of the cerebral vascular bed and consequently a cerebral hyperperfusion during hypoxia (16). If the oxygen deficit is continued the cardiac output and the mean arterial blood pressure will fall and the cerebral perfusion will decline. If the oxygen supply is restored a cerebral hyperperfusion will follow in response to the postasphyctic increase in cardiac output. The initial hyperperfusion of the brain is followed immediatly by a phase of hypoperfusion that might be due to release of free oxygen radicals (17). The phase of hypoperfusion will eventually recover or even develop into a new phase of hyperperfusion extending over in the phase of second energy failure. The latter is often accompanied by an isoelectric electroencephalogram (EEG) and this combination is signaling a very unfavorable prognosis (18). In some cases, a so-called no-reflow phenomenon can be observed regionally or generally in the brain after severe cerebral ischemia, due to congestion of cerebral vasculature.

This description of vascular changes of perinatal hypoxia ischemia is however schematic, simplified and based on experimental animal studies of various species, with limitations and differences compared to human babies.

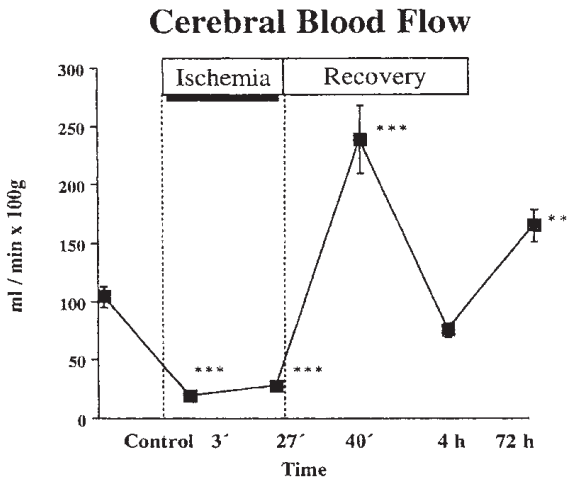

Fig. 1 The effect of ischemia on cerebral perfusion, Berger et al (13)

As opposed to adult stroke, being in most cases mainly ischemic, in the perinatal situation the combination of hypoxia and ischemia is more common. In adult HI injury/ stroke the concept of "penumbra" is defined as tissue with flow within the thresholds for maintenance of function and of morphologic integrity with a capacity to recover if perfusion is improved (19). Significant gaps still exist in our knowledge of pediatric CBF and its relation to the time for and cause of HI brain injury, as well as regional cerebral changes related to the degree of hypoxia-ischemia.

Very few modalities exist for easy monitoring of CBF in high-risk neonates. Near-infrared spectroscopy (NIRS) can monitor microvascular cerebral oxygenation deducing CBF from changes in total hemoglobin concentration. NIRS is used during cardiothoracic operations, postnatally after a HI event and in premature babies with ventilatory problems to prevent cerebral periventricular leucomalacia (20). Although the clinical use of NIRS has expanded, most devices available are limited to quantify only relative changes in CBF (21).
Transcranial Doppler can be used to measure CBF velocity in major intracerebral arteries but is limited to only short periods of assessment to avoid high power transmission over a long time (22). Recent advances in non-invasive MRI techniques provide novel techniques to evaluate neonatal CBF but they are still not bedside techniques suitable for monitoring in clinical practice. Under experimental conditions, radioactive, colored or fluorescent microspheres have been used for decades and this is the current gold standard technique for detection of regional CBF changes (23).

Glucose metabolism in HI injury

Like perfusion, cerebral metabolic demand and neuronal function are crucially involved and important for the evaluation of HI brain injury and recovery. The ischemic cell damage involves a cascade of molecular and biochemical mechanisms where glucose and oxygen metabolism are closely involved.

Glucose metabolism has regional differences in the brain. Thalamus, cerebellum and brainstem, sensorimotor cortex and basal ganglia, have higher metabolic activity than frontal, temporal and occipital cortex and white matter (24;25). These areas of the brain which have the highest concentrations of glutamate or other excitatory amino acid receptors, are more likely to excitotoxic injury during HI (14). Excitotoxic injury or excitotoxicity, refers to cell death caused by excessive stimulation of extracellular excitatory amino acid receptors (26). The degree of brain maturity also influence on glucose metabolism (27). Premature babies less than 32 weeks of gestational age have decreased glucose metabolism compared to term infants as shown in a recent study (24;28).

During the early phase (3-12 h) of the evolving HI injury, areas with increased cerebral metabolism of oxygen and glucose have been detected in animal studies (immature rats) and and also in relation to CBF changes (29-31). Also in term infants, hypermetabolism was found a few days after hypoxia-ischemia correlated to poor outcome (32). Marginally ischemic tissue has been revealed to have a higher fraction of anaerobic glycolysis than normal tissue and represents areas in danger of developing infarction (33). The mechanism of hypermetabolism could be partly due to the action of excitatory amino acids released following HI and this hypermetabolic state may precede irreversible infarction later presented as hypometabolism.

Patterns of injury

In HIE, the time of the insult, the duration and the severity in addition to the degree of cerebral maturation and regional metabolic state of the brain, play a key role for the development and pattern of the resultant cerebral injury. Most episodes of hypoxia-ischemia severe enough to damage the brain cause variable injury to selected groups of structures rather than an uniform or global injury, often seen in adult anoxic ischemic injury. Special patterns of injuries corresponding to clinical patterns of disability have been revealed especially by neuroimaging, such as MRI.

In term babies subjected to mild to moderate hypoperfusion/hypotension, the CBF is redistributed to ensure perfusion to the hypermetabolically active and most vulnerable

regions including the basal ganglia, brainstem, and cerebellum. This redistribution results in injury predominantly to the intervascular zones of the cerebrum between the anterior, middle and posterior cerebral arteries, in the underlying subcortical white matter in parasagittal locations. In severe hypoperfusion/ hypotension, the vulnerable regions of the brain affected are: the deep gray matter including lateral thalami, posterior putamina, hippocampi, brainstem, corticospinal tracts and sensorimotor cortex (34;35). This pattern is commonly associated clinically with severe permanent motor impairment (upper extremities more than lower extremities) and motor speech impairment.

5.1.3 Resuscitation after hypoxia-ischemia

The supportive care provided postnatally following asphyxia aims to avoid circulatory insufficiency and cerebral hypoperfusion. Resuscitation is often needed and ventilatory support is one of the initial steps together with fluid management and measures to avoid hypotension and hypoglycaemia as well as treatment of seizures.

Oxygen is the key element of aerobic metabolism. Its reduction to water by the mitochondrial transport chain enables the conversion of ADP to ATP in an 18 times more efficient way than by glucolysis. Oxygen has been used in neonatal resuscitation since 1780, but it took over 200 years before it was suggested that it could be harmful when used in newborn resuscitation (36).

In 1980 Saugstad and Aasen introduced the theory that oxygen free radicals could cause injury during hypoxia and reoxygenation, proposing that care should be taken when using pure oxygen during resuscitation (37). Since then the concentration of oxygen in the resuscitation air has been under extensive experimental and clinical research to establish the long- and short-term effects of high-level oxygen. There has been an on-going debate regarding the potentially harmful effects of oxygen free radicals and changes in cerebral perfusion and respiratory physiology with 100% oxygen administration, but also about the dangers of oxygen deprivation during and after asphyxia. Animal studies now show convincing evidence that oxidative stress may, induced by hyperoxemia, lead to inflammation and necrosis/apoptosis in the brain, as well as in other organs with potential negative effect on survival (38-40) . Clinical studies also show that hyperoxic compared with normoxic reoxygenation of newborn infants leads to organ tissue injury, for instance in the myocardium and kidney (41). Consequently the International Liaison Committee on

Resuscitation (ILCOR) recommends in their new guidelines, to start with air in resuscitation of term or near term newborn infants (42).

Hyperoxia has been shown to cause reduced CBF. This hypoperfusion has been observed after neonatal HI injury, but the mechanism is not fully understood (17). A study in newborn babies could demonstrate reduced CBF (using xenon clearance) after hyperoxia shortly after birth (43). An experimental study on newborn rats (7 days) showed that CBF in the ischemic cortex declined following resuscitation with 100% O_2 but not with ambient air. These findings in hyperoxic animals were accompanied by reduction in perivascular production of nitric oxide (NO). The authors suggest that hyperoxia uncouples perivascular NO synthase (NOS), probably endothelial NOS, leading to a reduced NO and increased superoxide anion (O_2^-) production. The hyperoxia causes a loss of vascular reactivity initiated by a decrease in the production of perivascular NO and an increase of oxygen with vasoconstriction resulting in reduced CBF (44). However newborn piglet studies have revealed that hypoxia-ischemia combined with hypercapnia and hyperoxic resuscitation resulted in a faster restoration of cerebral microcirculation than with normoxia, suggesting that hypercapnia may have protective effects (16).

The effect of hyperoxia versus normoxia on cerebral glucose metabolism in perinatal HI injury has not been compared in the previous studies. An experimental study in fetal sheep revealed a pronounced hypometabolism 4 h after hypoxia-ischemia and resuscitation with 100% O_2 (45).

5.1.4 Cerebral injury and neuroprotective treatment

Detection of injury - the importance

Resuscitation and early treatment will most often be initiated by the suspicion of perinatal asphyxia, which can only later be confirmed by a combination of developing clinical symptoms, biochemical markers together with EEG and neuroradiological findings. HI injury develops during the first days of life and is classified according to a system based on clinical and EEG findings as first described by Sarnat and Sarnat in mild, moderate or severe HIE (46).

Therapeutic treatment has become a reality in infants born at term or near term who have suffered perinatal hypoxia-ischemia (9;13;47;48). It is important that this treatment is started during the early recovery period, only 2-6 h after the insult, before the permanent brain injury is established. Hence, it is crucial to evaluate various methods, including

imaging and the use of biomarkers, to assess the viability of cerebral tissue early after birth, in order to select the infants with the highest risks of developing brain injury after asphyxia, and those that could benefit from neuroprotective treatment.

Neuroprotective treatment

Until recently, the management of a newborn with encephalopathy has consisted largely of supportive care to restore and maintain cerebral perfusion, provide adequate gas exchange and treat seizure activity.

Recent randomized controlled trials have shown that mild therapeutic hypothermia initiated within 6 h of birth in moderate to severe HI injury reduces disability and may reduce death in these infants (49-51). Hypothermia is the most promising treatment for HI injury. Still, in the clinical trials more than 40% of the treated infants died or survived with severe impairment (48;52). Thus, other neuroprotective interventions that could act synergistically or additively need to be investigated. Promising results have been found in animal models with different agents like xenon, magnesium, calcium blockers, melatonin and recombinant erythropoietin but further clinical trials are needed (48;49).

Further knowledge of the early mechanisms of asphyxia leading to injury is of great importance for early detection of viable and injured tissue and start of neuroprotective treatment.

5.2 Neuroimaging of cerebral HI injury – current challenges and new techniques in ultrasonography (US), magnetic resonance imaging (MRI) and positron emission tomography (PET)

Assessment of cerebral injury can help to predict the outcome of the HIE (53). However, to assess the viability of cerebral tissue early after the HI event in the clinical setting is extremely difficult since most techniques used in clinical routine do not provide that information. Techniques that do allow assessment of physiological parameters like PET, single photon emission computed tomography (SPECT), Xenon computed tomography (Xe CT), MRI with diffusion- (DWI) and perfusion weighted imaging (PWI) and MR spectroscopy (MRS) are until now logistically complex and not well suited for routine applications.

Of the neuroimaging techniques that have been proposed for investigating cerebral HI injury, MRI and US are considered the most important for diagnosis and prognosis (22;35;54). Transfontanellar US is a routine technique easy to perform bedside in the neonatal intensive care unit. Grey-scale, spectral- and color Doppler are used to detect parenchymal injury, as well as vascular anatomy and blood flow in detection of HI injury in the basal ganglia and cerebral cortex. However, the technique is operator dependent and shows only subtle changes, which may in most cases only be visible some days after the event. Until now, regional changes in brain perfusion have been difficult to detect with Doppler examination in the newborn.

MRI is considered the most sensitive and specific method to diagnose and predict HI by conventional sequences, DWI, PWI and MRS. Restricted diffusion corresponding to areas of cytotoxic edema has been shown already a few hours after the injury while spectroscopy may show increased lactate and reduced N-acetyl aspartate in the affected areas (47;53;55). However, the interpretation of the different image sequences can be difficult due to the fact that the time of the HI injury is often unknown and the time course of changes may be different from adult HI injury. MRI is unfortunately an expensive, time-consuming method that often requires transport to the MR unit and often sedation of the critically ill babies. MRI is often not performed until a few days after birth.

PET is a nuclear medicine technique that can be used to measure brain blood flow, oxygen and glucose metabolism. Early changes in glucose metabolism may be a prognostic indicator of perinatal brain injury after HI (25;32;56). As for MRI, it is difficult to perform a PET examination shortly after the insult, requiring transport of the baby to the PET scanner and current techniques for metabolic quantification in human babies are challenging.

Most human studies involving MRI and PET have been performed a few days after birth. A few animal studies on rats, sheep and piglets investigate the morphologic, metabolic and diffusion changes hours after the insult (10;31;45;57).

Neuroimaging experience of the evolution in perfusion and metabolic changes early after perinatal HI and resuscitation related to the ultimate injury is currently limited in animals and lacking in human studies.

5.3 Contrast enhanced ultrasonography (CEUS) - perfusion imaging

The introduction of new ultrasonographic contrast agents (CA) based on microbubbles has opened new possibilities in US diagnosis and real time non-invasive quantification of tissue perfusion. The CA dramatically increases the signal intensity from blood and is thereby enhancing the US signal.

Sulphur hexafluoride (SonoVue™, Bracco S.P.A™, Milano, Italy) is a CA of the second generation consisting of microbubbles (2-6 μ) containing a gas, sulphurhexafluoride (SF_6) stabilized by a shell (fig.2).

The SF_6 is an extremely stable and inert molecule that does not react with other molecules within the body and has been shown to be too small to cause vascular obstruction or other damage to the brain microcirculation (58). SF_6 is eliminated from the body by exhalation through the lungs.

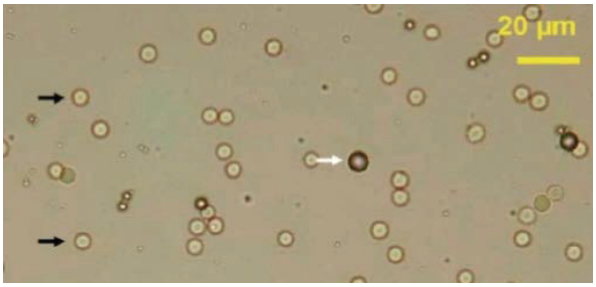

Fig. 2 Two-dimensional microscopic photo of SonoVue™ (white arrows) microbubbles (20× magnification; optical microscope) compared to red blood cells (black arrows). *(www.springerimages.com.)*

The response of the microbubbles to the sound field mainly depends on the insonation power, i.e. the amplitude of the acoustic pressure wave called the mechanical index (MI). At very low insonation power, the microbubbles remain static, simply reflecting (or more correctly, backscattering) the sound wave. At slightly higher acoustic pressures, the microbubbles start to oscillate at their resonance frequency resulting in the emission of specific sound waves. These waves can be detected by the US transducer as contrast-specific signals (59). If the acoustic pressure becomes too high, this oscillation becomes so strong that the membrane disrupts and the microbubbles are destroyed.

To be able to detect these backscatter signals a special software program within the US equipment is applied. For Acuson Sequoia 512™ (Siemens™, Erlangen, Germany) used in

our study (Paper II) the Contrast Pulse Sequencing (CPS) Cadence program (1.5 MHz) is switched on with a low frequency and MI.

There are two main strategies for contrast-specific imaging: 1. static, destructive imaging called *high-MI imaging* where burst/replenishment kinetics will evaluate the refilling of microbubbles after transient local destruction of microbubbles and, 2. continuous non-destructive imaging called *low-MI imaging* (MI ≤ 0.1). SonoVue™ is an optimal agent for low-MI imaging (soft, flexible shell and high stability), where the bubble destruction is minimized allowing continuous real-time assessment of the whole enhancement period.

CEUS provides qualitative perfusion estimates of a 2D scanned sector of the organ. Software programs are used for quantitation of parenchymal perfusion where the approach of classical bolus kinetics provide parameters, such as the peak intensity (PI) and the time-to-peak (TTP) area under the curve (AUC) and slope of the curve, after a fast bolus injection. Since SonoVue is an intravascular tracer, relative cerebral blood volume (rCBV) can be estimated from the AUC of the first-pass time intensity curve (TIC) and relative CBF (rCBF) from the PI of the TIC.

SonoVue™ is approved for clinical use in adults only and few clinical studies in children have been performed (59-62). Relatively few adverse reactions have been reported and no more than with other radiological CA (58;62;63).

Studies with CEUS in adults and animals have shown promising results in detecting and quantifying regional cerebral perfusion changes due to ischemia in the brain (63-66). CEUS has even been used for therapeutic thrombolysis in animal stroke (67). A few animal studies have been able to show changes in blood flow maps during normo- and hypercapnia in the newborn piglet brain (68;69).

5.4 MRI

Clinical MRI uses the magnetic properties of hydrogen (^{1}H) and its interaction with both a large external magnetic field and radio waves to produce highly detailed images of the human body.

MR imaging is based on the work by Bloch and Purcell showing that a nucleus with a spin momentum (spin) can interact with a magnetic field. This interaction is known as the nuclear magnetic resonance. The ^{1}H atom has only one proton as a nucleus and its spin can be observed. ^{1}H exists in water and fat, which are the main components of our body. The varying molecular structures and the amount of hydrogen in various tissues in the body,

affect how the protons behave in an external field. By placing the patient in a large external magnetic field, we magnetize the tissues (hydrogen), preparing it for the MR imaging process. Radiofrequency fields then systematically alters the alignment of this magnetization. This causes the nuclei to produce a rotating magnetic field detectable by the scanner. This information is recorded to construct an image of the scanned area of the body. MR imaging has five variables for tissue characterization – the proton density of the tissue, T1 and T2 relaxation times of tissue, flow and spectral shifts from which an image is constructed. These variables can be combined in various ways by selecting pulse sequences and pulse times to emphasize any desired combination of tissue characteristics in the image (70). Multiple planes can be chosen for imaging of the body. Of the clinically available imaging techniques, MRI has the highest spatial resolution and soft tissue contrast for detecting lesions in the brain and has become a very important tool in the detection of focal cerebral disorders in particular the neonatal brain and HIE.

5.4.1 Conventional MRI sequences

Conventional MR spin echo sequences based on proton density, T1 and T2 relaxation times, are less sensitive than newer techniques in revealing an ischemic injury in neonates within the first few hours and days following the ischemic event. At this early time point, it can be very difficult to detect abnormalities on either T1 or T2 weighted images. Common findings after 1-2 days are lesions with hypointense signal on T1- and hyperintense on T2 weighted images. After 3-5 days the signal becomes hyperintense on T1- and of variable intensity on T2 weighted images. These changes occur in the basal ganglia, hippocampi, corticospinal tracts including the perirolandic gyri but mainly sparing the remaining cortex. Injury to white matter generally results in low signal intensity on T1- and high signal intensity on T2 weighted images, due to ischemia-induced edema (34;71-73). In mild and moderate cases of hypotension, the MRI findings are mainly distributed in the parasagittal region. The assessment of conventional MR images can be difficult since the precise time of injury is often unknown. T1- and T2 weighted imaging findings at the end of the first week after birth are excellent in demonstrating permanent brain injury, while early prediction of the outcome based on T1- and T2-weighted images remains difficult (54;55).

5.4.2 Perfusion weighted imaging - dynamic susceptibility contrast (DSC) enhanced MRI

PWI is a collective term describing methods for deriving tissue blood flow or perfusion related parameters from MR images (74). These methods are based on the principle that a CA serving as a blood tracer affects the MR image signal intensity over time and can be related to tissue perfusion, blood volume or both. There are alternative methods based on completely non-invasive tracers such as arterial spin labeling (ASL) (75;76) but in this thesis the focus is on perfusion imaging by intravenous injection of a MR compatible CA – DSC-MRI.

DSC-MRI is based on the local changes of the MR signal in the tissues, where a CA is distributed. The CA alters the biophysical properties of tissue by increasing the proton relaxation. When the CA is injected as a rapid bolus intravenously, a dynamic image intensity curve as function of time can be related to blood flow, requiring the MR image intensity to be monitored with sufficient temporal resolution. In DSC echo-planar imaging (EPI) can be combined both with T2 weighted spin echo (SE) or/and T2* weighted gradient echo (GE) sequences. They are used to measure the susceptibility effects of the intravenous bolus injection of the paramagnetic CA, causing MR signal changes.

The EPI technique is very sensitive to T2* effects of the CA but also to other unwanted susceptibility effects present in the brain, which can cause signal loss and image distortion. In this thesis, the GE EPI sequence was used for the study in Paper II, in order to record stronger susceptibility effects from the CA in the small piglet brains where minor flow variations were expected.

Tracer kinetic modeling

Functional information can be derived using a blood tracer. Multiple hemodynamic parameters can be estimated from temporal characteristics of the first-pass time course of the CA (77). The MR signal intensity change versus time curve is converted by a pixel-wise analysis to a CA tissue concentration time curve derived from the first-pass CA response curve. Different quantitative maps can be created for different cerebral hemodynamic parameters: CBF (ml) CBV (ml/100g of tissue), mean transit time MTT(s) and TTP(s). These parameters are linked by the following relationship:

$$CBF \times MTT = CBV$$

A nonparametric deconvolution technique (singular value deconvolution) is used to estimate flow parameters from the time course of T2* weighted signal change in tissue and blood, following injection of the CA as first proposed by Østergaard and Wu (78;79). A linear relationship is assumed between the 1/T2* changes and the CA concentration in tissue and arteries. The arterial input function can be detected in pixels of a representative cerebral artery. rCBF can be obtained as the maximum value of the residual function obtained by deconvolution. rCBV is aquired by the AUC of the concentration time curves obtained from numerical integration between user defined time points (corresponding to arrival of CA in the ROI and the end of first pass). To eliminate contribution of tracer recirculation, a gamma-variate function is generally fitted to the measured raw concentration-versus-time curves.
To achieve good quality images of cerebral perfusion studies, adequate quantity of CA is needed and should be injected at a high flow rate preferably with a power injector (80). With increasing magnetic field strength, the signal increases, but also the artifacts of inhomogeneity thus challenging the image quality and calculation of hemodynamic parameters.

Although commonly used in adult neuroradiology, DSC-MRI is known to be technically difficult to perform in neonates and is not routinely used in the diagnosis of perinatal hypoxia. A few studies using DSC enhanced MRI, have reported reproducible and feasible techniques with perfusion patterns of injury in babies a few days after HI (80-83). They suggest that microvascular perfusion changes could be an important marker for identifying future ischemic areas. Reasons for the limited use of MRI in neonates however, include expensive and time-consuming examinations needing sedation and transport of an unstable critically ill neonate to the MR unit and the use of CA. The small doses of gadolinium CA recommended for babies are challenging to administer as a bolus injection with high flow rate. Regarding gadolinium CA, caution should be taken in patients with impaired renal function for the risk of development of a rare but devastating disease, nephrogenic systemic fibrosis (84). These precautions extend especially to neonates due to their immature renal function. The use of cyclic non-ionic gadolinium agents is recommended. Gadobuturol is one of the recommended CAs often employed for the MR perfusion, although not approved for use in children less than 7 years of age. These considerations make techniques like ASL an attractive alternative to DSC especially in pediatrics and a few studies have been reported

in infants and perinatal HIE (75;85). This technique was not available at the 3T MR unit at the time of our study (Paper II).

5.4.3 Diffusion weighted imaging (DWI) and Diffusion tensor imaging (DTI)

The term molecular diffusion refers to thermal Brownian molecular motion (86). In biological systems water diffusion occurs within and around cells with exchange between the intra- and extracellular space. Tissue water diffusion is restricted by intracellular structures and cell membranes.
Diffusion weighted MRI is performed using a single shot SE EPI sequences using pulsed diffusion gradients. The strength of the diffusion gradient is expressed as a "b" value in units of seconds per square millimeters. MRI diffusion is quantified by the apparent diffusion coefficient (ADC) which provides a measure of random water diffusion and depends on the direction of diffusion within tissues and varies with both overall water content and cellular location (87). To require an ADC map, at least 2 orthogonal diffusion measurements are needed. The ADC map quantifies the degree of restricted diffusion.

DWI can detect the self-diffusion of water as one of the first elements in the pathophysiologic cascade leading to ischemic injury (19). After severe ischemia, there is an increase in DWI signal as a response to the redistribution of water from extracellular to intracellular space, corresponding to a restricted diffusion. This disturbance in water-ionic homeostasis occurs immediately with disruption of perfusion. DWI can detect this very early signs of ischemia within minutes after arterial occlusion caused at least partly by cellular swelling or cytotoxic oedema (88). Diffusion restriction can be reversible with early recovery of perfusion.

In adult neuroimaging, the combination of DWI and PWI is used in the diagnosis of ischemic stroke (89-91). Decreased diffusion may be visualized on the ADC map while PWI can demonstrate the areas of perfused tissue. The areas of perfusion diffusion mismatch correspond to the "penumbra" representing the ischemic but viable tissue (perfusion within the thresholds of functional maintenance and morphologic integrity) that could be salvaged by timely reperfusion. This must be distinguished from areas of irreversible infarction (19).

In perinatal asphyxia, few studies have used the combination of DWI and PWI for the detection of injured tissue at risk and all have been performed a few days after birth (82;83). In a piglet study a combined reduction of ADC and PWI during hypoxia-ischemia was shown to be reversible 30 min after reperfusion (57). ADC that is reduced in the hyper-acute phase following an HI event may underestimate the final extent of injury (92). The role of DWI in the prognosis and outcome of HI injury, as well as the optimal timing for imaging is discussed by Rutherford (93). ADC values seem to be more reliable between the second and fourth day. At the end of the first week, DWI is less sensitive than conventional MRI to perinatal brain injury because of the transient pseudonormalisation of DWI. However, independent of the timing of the exam, DWI seems to be an objective method for confirming HI tissue injury. Rutherford et al have shown that in the basal ganglia/thalamus and in white matter ADC values $< 0.8 \times 10^{-3}$ /mm^2/s and $<1.1 \times 10^{-3}$ /mm^2/s respectively were shown to always be associated with infarction (93). A recent retrospective study concludes that the combination of findings on conventional MR sequences and ADC or MRS has a better prediction of outcome of term babies than MRI alone (94).

Diffusion tensor imaging (DTI)

Molecular diffusion is in fact modulated by the spatial orientation of large bundles of myelinated axons running in parallel through brain white matter. This feature can be exploited to map out the orientation in space of the white matter tracks and to visualize the connections between different parts of the brain on an individual basis. DTI gives information on apparent diffusion and diffusion anisotropy, related to brain maturation and alterations in the white matter pathways caused by HI injury (95;96). The complexity of the developing brain connectivity can be assessed in the preterm brain using diffusion tensor tractography where involvement of sensorimotor pathways and disruption of connectivity between thalamus and cortex can be shown in children with periventricular leucomalacia. Fractional anisotropy (FA) values may increase in the early phase after HI but with poor correlation to ADC values (97). A decrease of FA values appears during the first week after severe to moderate HI and show improvement after hypothermia treatment (98). Furthermore, recent data suggest that diffusion MRI may also be used to visualize rapid dynamic tissue changes, such as neuronal swelling, associated with cortical activation, offering a new and direct approach to brain functional imaging.

5.5 Proton MR Spectroscopy (MRS)

In contrast to MRI, ^{1}H MRS analyzes signal of protons attached to other molecules. Proton (^{1}H) is the most common biological nucleus used for MRS although Phosphorus (^{31}P) MRS can study tissue energy metabolism detecting phosphocreatine, ATP and inorganic phosphate (P_{i}).

Whereas for MRI only a single peak (water) is being mapped, the output of MRS is a collection of peaks at different radiofrequencies (RF) representing proton nuclei in different chemical environments, proportional to the number of contributing protons. The phenomenon called *chemical shift* is caused by the fact that the same nuclei in different molecules (*e.g.* water or triglyceride) or in a different part of a molecule have a slightly different resonance frequency, due to the different electron density, which shield the static magnetic field to varying degrees. Thus, different signals seen in the spectrum correspond to distinct metabolites. The chemical shift is generally expressed in parts per million (ppm).

MR spectra are obtained by using a stimulated echo (STEAM) or a double spin echo (PRESS) sequence, with a single voxel (volume of sample) or multi voxel acquisition over the desired region (99). The major metabolites revealed by ^{1}H-MRS are; Choline (Cho at ~ 3.2 ppm, Creatine (Cr at ~3.0 ppm and N- acetylaspartate (NAA at ~ 2.0 ppm). Lactate (Lac) is sometimes detected in normal neonatal brain but at a low level (~ 1.3ppm). Numerous other resonances may be recorded including those from glutamate, myo-inositol and γ-aminobutyrate.

Proton MRS can provide information on timing and pattern of acute brain metabolite changes during the 2 first weeks after perinatal HI injury, where Lac and NAA are considered especially important (99). Lac is produced by anaerobic glycolysis. An increase may represent impaired cerebral energy production by oxidative phosphorylation. NAA is mainly neuronal and increases with neuronal development, while decreased NAA signal can represent neuronal loss (100). Unlike DWI, MRS performed in the first 24 h after birth is sensitive to HI injury and seems to be a more reliable method for detecting HIE in this early phase and for selecting infants that may benefit from early intervention (101). Increased levels of lactate in the region of the basal ganglia/thalami have been detected in neonates with subsequent poor neurodevelopmental outcome (102;103).

Most studies report metabolic changes as ratios of the peak area integrals of NAA and Cho (NAA/Cho) and NAA and Cr (NAA/Cr). Quantitative measurements of metabolite

concentrations in mmol /kg wet weight of brain tissue, is recommended and may improve the prognostic value of studies soon after birth (104). Determining metabolite concentration is however, very complicated, requiring brain signal calibration against a reference signal as well as a complex spectral fitting and is therefore not often performed in neonatal clinical practice (105).

5.6 Positron emission tomography (PET)

5.6.1 PET tracers

PET is a non-invasive nuclear medicine technique that can detect abnormalities in different organs based on disorders in the chemical function and/or receptor expression at the cellular level, related to glucose metabolism, blood flow, receptor binding, oxygen utilization and the protein synthesis, release and transport. PET can provide hemodynamic information with quantitative parameters including rCBV, rCBF, regional oxygen extraction (rOEF) and cell viability, but also proliferation and/or metabolic activity of tissues, regional cerebral metabolic rate of oxygen (CMR_{O2}) and of glucose (CMR_{gl}). These quantitative maps result from the use of different substances of biological interest labeled with positron emitting radioisotopes. PET tracers for CBF are $^{15}O_2$ (inhal), $C^{15}O_2$ (inhal) and $H_2{}^{15}O$ (iv). $^{15}O_2$ and $C^{15}O_2$ in inhalation allow measurement of CBV and CMR_{O2}.

PET radiopharmaceuticals are cyclotron products and have variable but generally very short half-life. The hybrid scanners with PET-CT can provide information on functional changes with anatomical correlation. Also PET-MR scanners are now commercially available.

5.6.2 Fluoro-deoxy-glucose positron emission tomography (FDG-PET)

In FDG-PET, regional glucose consumption is measured in living tissues for the evaluation of cancer with whole-body scanning. Additionally it is a reliable method to detect regional metabolic deficit in the brain. Using a labelled glucose analogue (^{18}F) 2-deoxy-2-fluoro-D-glucose (FDG), absolute quantification of regional glucose consumption can be performed after an adaptation of the (^{14}C) 2-deoxy-D glucose model, originally described and developed by Sokoloff and co-workers (106). Deoxyglucose and thereby fluorodeoxyglucose is believed to accumulate in active neurons reflecting the energy requirements of Na/K ATPase sensitive pumps (107). In HI injury both irreversible and marginally ischemic tissue may be detected by this technique (108). In human babies it is

difficult to perform a PET examination shortly after the insult, because this requires transport of the baby to the PET scanner. In addition the technique for metabolic quantification in human babies is challenging requiring repeated arterial blood samples and is not well developed. Single-scan, autoradiographic methods and measurement of relative metabolic changes have often been used for calculation, as well as semiquantitative analysis of cerebral glucose utilization - the Standardized uptake value (SUV). The latter is defined as tissue radioactivity divided by intravenously administrated dose per kg body weight of the patient.

The radiation dose is a drawback with this method especially regarding pediatric use. The European Association of Nuclear Medicine (EANM) recommends a minimum injected dose FDG of 3-6 MBq/kg to a newborn, corresponding to an effective dose estimated to be 2.9-5.7 mSv/kg (109). This radiation dose is quite considerable but still lower than a standard brain CT scan of a baby estimated to be of about 5-9.5 mSv (110).

Only a few and small studies of neonatal asphyxia and FDG-PET have been performed until now (25;28;32;107;111-114). However, small animal PET systems provide a superior spatial resolution compared to clinical human scanners and have the advantage of being portable and can be taken to the newborn nursery for scanning of the baby (56).

Dynamic PET analysis

CMR_{gl} values can be estimated from the dynamic FDG-PET series over time by a multiple time-graphical analysis , by an approach proposed by Patlak et al (115). This is based on a compartmental tissue model assuming irreversible trapping of the tracer. Here, plotting the ratio of the FDG tissue concentration C_{tissue} to the plasma concentration C_p versus the plasma FDG concentration time integral to $C_{p,}$, yields a curve that approaches a straight line at late time points post injection. The ratio, C_{tissue}/C_p, is often denoted "volume of distribution" while the latter is termed "normalized plasma integral". The Patlak equation is given by the expression:

$$\frac{C_{tissue}(t)}{Cp\ (t)} = K\ \frac{\int_0^t C_p(\tau)d\tau}{C_p(t)} + V_o$$

The slope of the line, K, is proportional to CMR_{gl}. V_0 equals the initial distribution volume (including the fractional blood volume). C_{tissue} is obtained from dynamic FDG-PET and C_p

from the arterial blood sampling. In order to obtain the cerebral metabolic rate of glucose, the lumped constant (LC), used to correct for the difference in metabolism between fluorodeoxyglucose and glucose in the brain, must be taken into account. LC varies for different species, age, studied organ and also change under pathological conditions (116). Together with b-glucose values *[Glc]* of the blood samples, CMR_{gl} is calculated according to the following expression:

$$CMR_{gl} = [Glc] \frac{K}{LC}$$

5.7 Other perfusion imaging techniques

Single photon emission computed tomography (SPECT) is a non-invasive technique generating tomographic images of the 3D distribution of a specific radiopharmaceutical, which may reflect regional cerebral hemodynamics, dopamine or other transporter distribution. The main indications are acute and chronic cerebrovascular diseases (head trauma), psychiatric disorders and presurgical localization of epileptogenic foci (117).
CT Xenon ^{133} Xenon enhanced CT has long been used for quantitative evaluation of CBF in humans. Stable non-radioactive xenon is inhaled and serves as a CA. The gas dissolves in the blood and crosses the blood brain barrier to the brain and CBF is calculated. The main clinical application is cerebrovascular disorders, to provide measurements of equal validity in the cortex and deep structures and determine the ischemic threshold. The short half-life of inhaled xenon makes Xe CT suitable for repeat CBF measurements (117).
Dynamic Perfusion CT like DSC-MRI uses first pass tracer methodology following intravenous bolus injection of iodinated CA to measure brain hemodynamics. CBF, CBV, and MTT can be measured and visualized by parametric maps. The advantage is short imaging times (<10 s) and widespread availability in the emergency setting. Perfusion CT can rapidly detect the size of hypoperfused regions (penumbral tissue) in cases of acute stroke, vasospasm following subarachnoid hemorrhage (118).
The radiation burden is considerable in all the mentioned techniques and careful selection of indications is warranted, especially in pediatrics even though bedside use is possible.

5.8 The piglet model for studying HI

In all animal studies, ethical considerations must always be taken and as a rule all efforts must be made to:

- Reduce the number of included animals as much as possible while retaining the scientific requirements for statistical analysis.
- Refine the models to minimize the group sizes while maximizing the quality of acquired information.
- Replace in vivo analysis by in vitro models whenever equivalent information can be obtained. This has not been possible for this thesis.
- Relieve animals from any distress by careful handling and adequate analgesia and anesthesia when needed.

In our studies, all the experimental protocols were approved by the Oslo University Hospital's ethics committee for animal studies under the surveillance of the National Animal Research Authority, and performed by certified category C researchers of the Federation of European Laboratory Animal Science Associations. We have studied 12-36 h old Noroc pigs. They were delivered from the farmer on the day of the experiment in a warm incubator, remaining as long as possible with the sow to avoid stress and dehydration. Exclusion criteria: a reduced general condition, wounds, dehydration, Hb < 5g/dL and a weight < 1600g.

The accessibility of a well-controlled animal model for investigating neonatal injury due to hypoxia-ischemia is of great importance. It is difficult to study the pathophysiology of perinatal asphyxia in human babies and much of our understanding concerning neonatal HI injury originates from animal studies.

When choosing an animal model it is important to consider the differences between species regarding O_2 response, different biochemical responses, lack of reference values for common functional variables and different cerebral maturation at birth. The resemblance to the HI injury found in human babies is essential. For this purpose, the piglet is suitable and many studies over the last decades have gathered experience and data. The piglet has the size comparable to a newborn baby and the cerebral maturation and myelinisation of the newborn pig is comparable to the human neonate of 36-38 weeks of gestation, but its physiology is probably more mature (119). Newborn piglets have higher rates of cerebral

metabolism and CBF than humans do. The normal values of CBF decrease with age in contrast to humans. However, the hemodynamic and pathophysiologic responses to HI resemble the responses seen in human babies.

Animal models can never completely mimic the human perinatal conditions. The piglet model has several limitations. As human babies in the clinical setting, piglets are variable in their response to hypoxia. Some piglets are preconditioned to hypoxia in intrauterine life and some are more resistant to HI for various reasons. In the perinatal model often used, the period of transition from fetal to newborn circulation cannot be studied. Similar to humans, the PDA is functionally closed at 4-20 h after birth and the pulmonary pressures have already fallen at the time of the experiment.
The combination of hypoxia and ischemia or isolated ischemia is necessary for the development of brain injury (14). Different ways to induce asphyxia/ hypoxia-ischemia have been used. The Vannucci model often used in rodents, has been adapted for use in piglets (120). The occlusion of carotid arteries combined with low flow FiO_2 induces both local ischemia and global hypoxia (121). Other models use global hypoxia with variable or constant FiO_2 (16;122;123). Here ischemia can be induced when MABP falls below cerebral autoregulation for a longer period of time. In constant FiO_2 models MABP and BE have been used to monitor the animals and ensure adequate damage.

In our studies, we have used the two different models. In Paper I, both carotid arteries are clamped during global hypoxia with a constant FiO_2 0.08, until MABP <15 mmHg or Base excess < -20 mmol/l is achieved. A relatively severe brain injury is established by this model. In Paper II and III, global hypoxia was induced with a constant FiO_2 0.08 alone until MABP < 15 mmHg or Base excess < -20 mmol/l was achieved, or alternatively a total duration of hypoxia of up to 30-60 min. With this approach, the degree of injury may be more variable.
In the two studies, using the model of global hypoxia the goal was to establish a moderate brain injury, which in clinical practice is the most challenging in terms of early identification of injury. If the injury is too severe with early development of cell death and especially brain edema this would hinder perfusion and metabolic measurements.

6. Aims of the study

The aim of this study was to introduce and evaluate methods from radiology and nuclear medicine for use in newborn piglets to detect early effects and mechanisms of perinatal cerebral hypoxia-ischemia correlated to the degree of injury. The influence of high-level oxygen versus air in the resuscitation air was another goal of the study. Cerebral perfusion, diffusion and metabolism were measured by using CEUS, DSC enhanced- and DWI MRI and MRS. The glucose metabolism was measured by using FDG-PET.

Specific aims

1. To develop a piglet model where the MR techniques, MRS and DWI are used for early assessment of acute tissue changes in the piglet brain after hypoxia-ischemia. Our hypothesis was that this model is suitable to mimic human perinatal HI injury to be demonstrated with the MR techniques.

2. To quantify cerebral glucose metabolism and cerebral microvascular perfusion changes due to hypoxia and resuscitation. FDG-PET, DSC enhanced- and DWI MRI and CEUS were used. Can these techniques be adapted to study the newborn piglet brain?

3. Can DSC enhanced-, DWI MRI and CEUS detect early diffusion and microvascular perfusion changes respectively corresponding to early brain injury after global hypoxia and resuscitation?

4. To use a dynamic FDG-PET method to evaluate changes in cerebral glucose metabolism in the early phase after global perinatal hypoxia. Can PET quantify hypermetabolism after hypoxia?

5. How does the resuscitation strategy, using air (21% O_2) or hyperoxia (100% O_2), influence on cerebral perfusion, diffusion and the glucose metabolism after global hypoxia?

7. Summary of papers

Paper I. A piglet model for detection of hypoxic-ischemic brain injury with magnetic resonance imaging, Acta Radiol. 2008 Nov;49(9):1049-57

Purpose

To assess whether the use of a combined protocol including conventional MRI, DWI, DTI, and proton MRS can detect pathological findings in a piglet model 7 h after HI.

Material and methods

In this study, we used a piglet model of HI injury. Detailed description of the protocol is found in paper I. Ten piglets were subjected to hypoxia-ischemia for 30 min by FiO_2 0.08 in N_2, and bilateral clamping of the common carotid arteries and this was followed by 7 h reoxygenation with ambient air (21% O_2) and reperfusion. The occlusion of the arteries was verified by 2D ultrasonography with color and spectral Doppler. MRI was done prior to and 7 h after the hypoxia-ischemia.

Anesthesia was induced by sevoflurane 5% and replaced by an intravenous (iv) bolus injection of pentobarbital sodium 20 mg/kg and fentanyl 50 μg/kg iv. Anesthesia was maintained by a continuous infusion of fentanyl 50 μg/kg/h and midazolam 0.25 mg/kg/h. Tracheostomy was performed, and ventilation secured by a pressure-controlled ventilator at a rate of 30 breaths/min. Normal ventilation (arterial carbon dioxide tension [$PaCO_2$] 4.5–6.0 kPa, O_2 saturation ≥90%). FiO_2 and end-tidal CO_2 were monitored. After stabilization, the piglets were transported to the MRI suite in an incubator where anesthesia was maintained with a continuous inhalation of isoflurane (1–1.5% minimum alveolar concentration and a mixture of N_2O (30%) and O_2 (70%) and an hourly bolus injection of fentanyl 50 μg/kg. During the experiment, the animals were monitored measuring heart rate, peripheral O_2 saturation, end-tidal CO_2, and invasive blood pressure. Rectal temperature was maintained between 38 and 40°C. At the end of the experiment, the piglets were terminated by a dose of 150 mg/kg pentobarbital iv.

1.5T MRI was performed with 2D turbo spin-echo (TSE) T2-weighted images, coronal 2D fluid-attenuated inversion recovery (FLAIR) images, 3D SE EPI diffusion-weighted images, *b* values 0, 500, and 1000 s/mm^2, and 12-directional SE EPI diffusion tensor images, *b* value 750 s/mm^2. Single-voxel proton MRS (PRESS, TE/TR 270/1600 ms), was obtained from the basal ganglia, identifying the metabolites NAA, Cho, Cr and Lac.

MR analysis Morphological changes on T2- and FLAIR-weighted sequences were evaluated. MRS post processing was performed and the peak area ratios of NAA/Cho and NAA/Cr were calculated using integral values and the presence or absence of a Lac peak was recorded.

ADC- and FA maps were co-registered with conventional MR images and ROIs were drawn around the basal ganglia. Mean ADC and FA values for both time points were recorded.

Histology stained with hematoxylin and eosin (H&E) and microtubule-associated protein 2 (MAP-2) staining was performed in the basal ganglia at the end of the experiment. Necrotic areas showed loss of MAP-2 staining. The damage was reported as <10%, 10–30%, 30–60%, 60–90%, or >90%.

Statistical analysis the ADC and FA pixel values from the ROIs were compared for the two time points using a Student *t* test. Binary logistic regression was used to differentiate the ADC and FA values being best to differentiate between the time points. The differences between mean ADC, FA values and MRS ratios for the two time points for the piglets as a group were evaluated by Mann-Whitney tests. The correlation between the results from histology and MR was evaluated for the ADC- and FA values, and the presence of lactate (yes/no) using the Spearman rank-correlation coefficient (R_s).

Results

We found alterations in the basal ganglia with MRS and DWI confirmed by histology. Compared to baseline, ADC, NAA/Cho, and NAA/Cr were significantly reduced after 7 h ($P< 0.001$, $P= 0.01$, and $P= 0.05$, respectively) (fig. 3 and 4) and FA values were increased ($P< 0.025$). The ratios of Lac/Cho and Lac/NAA were significantly higher after 7 h compared to baseline ($P< 0.001$). Presence of necrosis correlated well with reduced ADC ($R(S) = 0.91$) and presence of Lac ($R(S) = 0.80$). Histology and MAP-2 staining showed more than 90% necrosis in eight piglets, 60% in one piglet, and no necrosis in one piglet. Diffusion MRI and proton MRS can detect HI injury in the piglet brain 7 h after hypoxia.

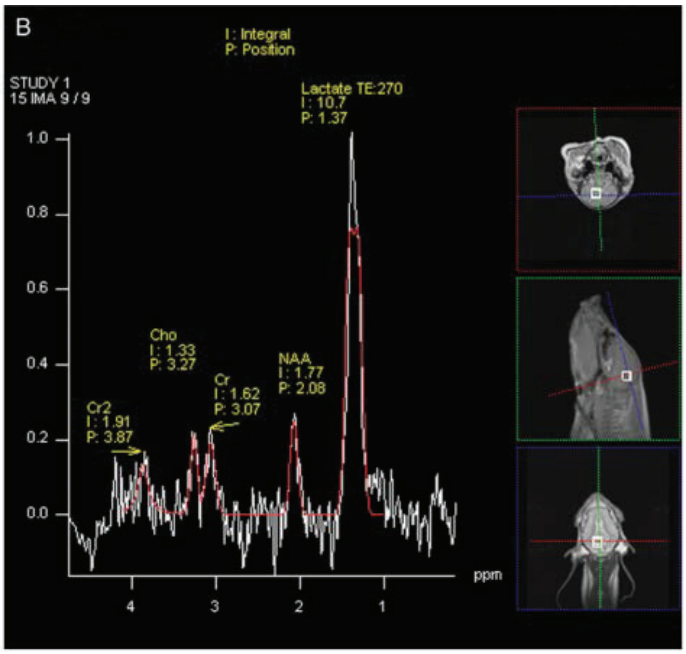

Fig 3. Proton MRS spectra (single voxel, PRESS) of a subject after 7 h. Integral (I) and position (P) values of Choline (Cho), creatine (Cr), N-acetyl aspartate (NAA), and Lactate (Lac) were recorded in the basal ganglia.

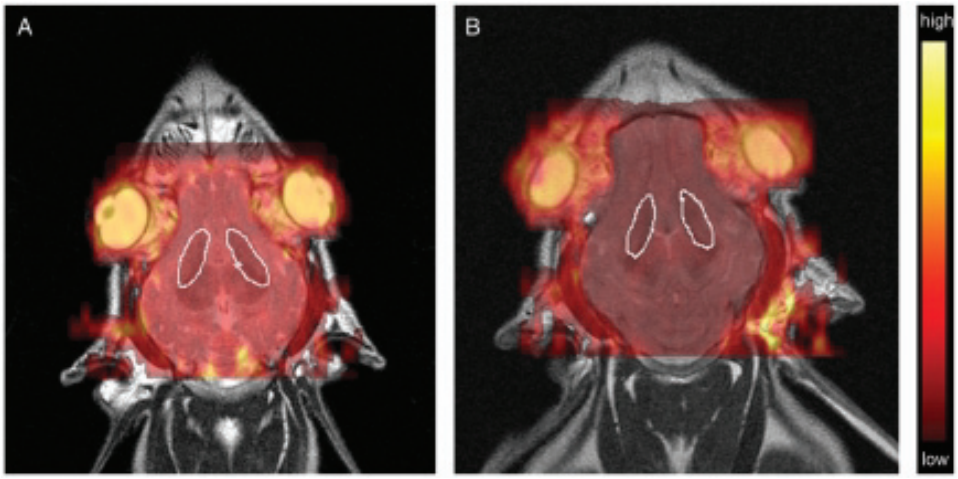

Fig 4. ADC maps co-registered with MR images, with traced ROIs in the region of basal ganglia before (A) and 7 h after hypoxia and resuscitation (B). High diffusion corresponds to yellow and restricted diffusion to dark red/ black, illustrated with the color bar.

Paper II. Cerebral perfusion in perinatal hypoxia and resuscitation assessed by Trans cranial Contrast Enhanced Ultrasound and 3T MRI in newborn pigs. Invest Radiol. 2011 Nov;46(11):686-96

Purpose

By further developing the piglet model from paper I, this study aimed to quantify microvascular perfusion changes due to hypoxia and resuscitation. CEUS, DSC-MRI and DWI were compared. Can these techniques detect early changes corresponding to brain injury after hypoxia and resuscitation?

Material and methods

Seventeen piglets were included in the study. After 1 h of stabilization 12 piglets were subjected to 30 min hypoxia, FiO_2 0.08 in N_2 and then randomized to 30 min of reoxygenation with FiO_2 0.21 (n=6) or FiO_2 1.0 (n=6) and then 7 h reoxygenation with air. Five sham-operated piglets served as controls. CEUS followed by MRI, was performed after stabilization immediately before the intervention. CEUS was performed after 10 and 25 min of hypoxia and after 15 min of resuscitation. CEUS followed by MRI was then performed after 30 min, 2, 5 and 7 h of reoxygenation.

Anesthesia is described in the summary of paper I and in paper II. Anesthetized and tracheotomized piglets were placed on a portable MR bench. They were transported in and out to of the next-door MR suite for each MRI exam. During the experiment, the animals were monitored measuring heart rate, peripheral oxygen saturation, end-tidal CO_2. Continuous invasive blood pressure recording in the abdominal aorta was assured by a MR compatible catheter via the femoral artery.

Fig. 5 Experimental setup, described below.

US examination Transcranial US with CEUS was performed, with a curved linear transducer (4V1S, 1-4 MHz) in a midline coronal plane, at the level of the basal ganglia and the internal carotid arteries (fig. 5).

CEUS The US-equipment was switched to CPS, Cadence. The frame rate was 17 Hz and MI= 0.16 with an insonation depth of 60mm. A bolus injection of SonoVue™ 0.2 mL (0.03 mg/kg bodyweight) in the internal jugular vein was administered followed by a flush of 2 mL saline solution. A 30 s image sequence was digitally stored.

CEUS perfusion analysis was performed with Axius Contrast Quantification™, by manual tracing of ROIs; in the internal carotid arteries, basal ganglia (BG) and parasagittal cortex in both hemispheres and one ROI of the whole brain. Subsequently the datasets for the TICs for the different regions were analyzed offline with an adapted software program (fig.6) The parameters TTP, PI, the upslope of the TIC named ” a” were estimated. The AUC was reported with values of the raw curve and of the gamma-variate fit curve. Since SonoVue™ is an intravascular tracer rCBV can be estimated from the AUC of the first-pass TIC and rCBF from the PI of the TIC. The parameters were recorded for the different ROIs and at 8 time points: prior to, early and late during hypoxia, during resuscitation and reoxygenation.

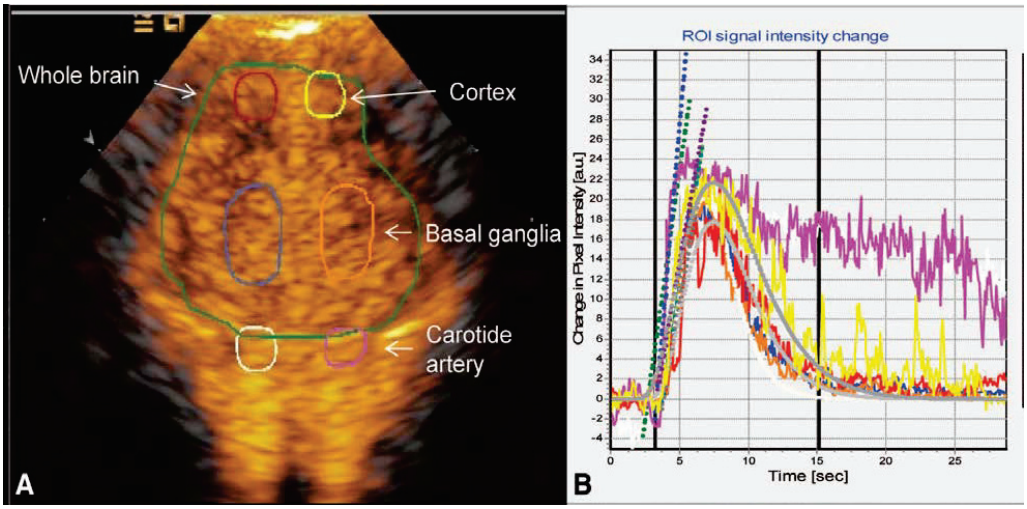

Fig 6. CEUS of a piglet brain in a coronal plane. A. Raw maximum intensity in Cadence mode, with the different traced ROIs. B, Corresponding TICs with gamma fit. The violet and white ROIs in the internal carotid artery and the corresponding TICs showing recirculation of the microbubbles.

3T MRI was performed after the US examination at five fixed time points with sagittal 3D TSE T2-weighted images and coronal 2D T1-weighted inversion recovery images. DWI was derived from SE EPI diffusion tensor sequence with b-values of 0 and 1000 s/mm^2 applied in 15 directions. DSC-MRI was performed using a GE EPI sequence acquired in an axial plane with 60 dynamic scans. Gadobuturol 0.2 mmol/kg was injected as a bolus by hand followed by 9 ml of saline solution.

MR analysis Morphological changes on T1/T2-weighted images were evaluated as in Paper I. For the MR perfusion analysis, maps of rCBF, rCBV and MTT were created from pixel-wise analysis of the CA concentration time curve derived from the first-pass CA response curve. The non-parametric deconvolution technique (singular value deconvolution) was used to estimate flow parameters from the time course of T2* weighted signal change in tissue and blood following injection of the CA. The arterial input function was detected near the anterior cerebral artery.

For diffusion analysis, ADC maps were generated from the diffusion tensor images, rCBF, rCBV, MTT, and ADC maps were co-registered with the conventional MR images, and ROI's were manually drawn around the basal ganglia, the parasagittal cortex, the central sulcus in each hemisphere and of the whole brain (fig. 7). The mean values of rCBF, rCBV, MTT, ADC at the five time points were recorded. All perfusion/diffusion analysis and image co-registration were performed using the same software program as for CEUS analysis.

Histopathology Fixation, staining and immunohistochemistry were performed as in paper I.

Statistical analysis Differences in the values of mean arterial blood pressure and heart rate in the hypoxia group were compared between baseline and hypoxia with paired samples t-test. The diffusion and perfusion changes were evaluated for MR and CEUS for the piglets as a group, depending on the type of resuscitation (six piglets in each group) and histological outcome compared to controls (n=5). Baseline values were compared to those at time point 2-5 in MRI and corresponding time points 2-8 in CEUS using linear mixed model, with a significance level of p= 0.05. The difference between mean values at each time point for the piglets compared to the controls was evaluated by Mann-Whitney test. The relationship between the results from histology and MR and CEUS was evaluated for ADC, rCBV, rCBF, MTT and PI, TTP, AUC raw/gamma and upslope a.

Results

We found in CEUS, compared with the control group, that perfusion changed significantly over time, in the hyperoxic group in all regions for PI, AUC in all regions of interests. The changes presented mainly as decreased perfusion during and shortly after resuscitation, for PI in the BG, cortex, and the whole brain with 50 to 60% ($P \leq 0.001$). A decrease was also found for AUC in the BG (fig. 8) and cortex with 90% ($P \leq 0.02$) and in the whole brain with 70% ($P = 0.004$). In the injured brains (confirmed by histology), significant changes over time were seen in TTP and AUC with mainly increased perfusion during late hypoxia. This increase was seen for TTP in the cortex, AUC in the BG and whole brain with 90 to 100% ($P \leq 0.04$), and for TTP in the whole brain with 50% ($P = 0.02$). DSC-MRI showed the same trends as CEUS in perfusion with regard to relative CBV. In all piglets exposed to hypoxia, perfusion returned toward baseline values at 7 h after hypoxia in both methods. ADC decreased significantly after 7 h in the injured brains in the BG from $114.6 \pm 1.2 \times 10^{-5}$ mm^2/s to $90.3 \pm 24 \times 10^{-5}$ mm^2/s ($P = 0.03$).

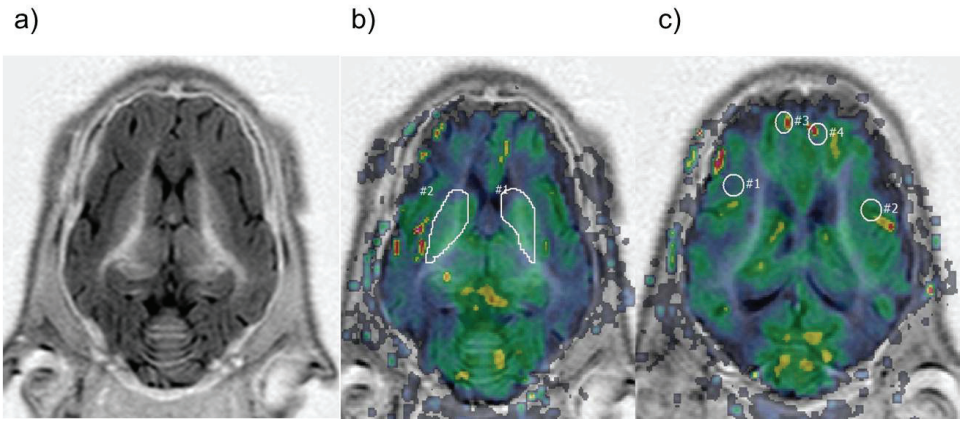

Fig. 7 MRI, axial T1 weighted image at baseline a), DSC-MRI CBF map with ROIs around the basal ganglia b), and in the cortex c).

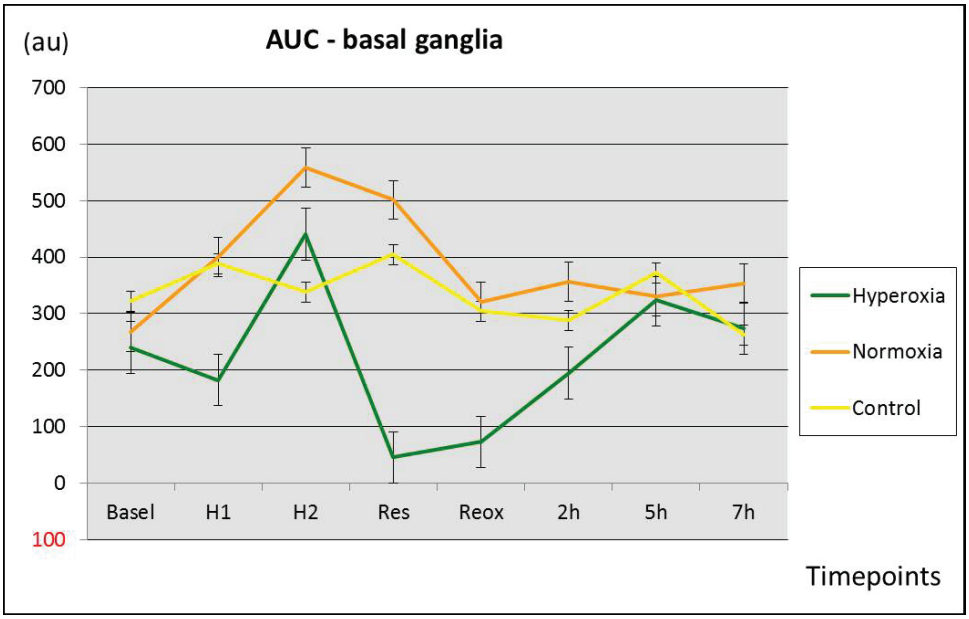

Fig. 8 CEUS - Evolution of AUC. a) Values (with SD error) in the basal ganglia over 8 different time points for the piglets as a group resuscitated with 21 or 100% O_2 compared to the controls. Increased AUC is seen during hypoxia and marked decrease during resuscitation in the hyperoxic group.

Base=baseline, H1=early hypoxia, H2=late hypoxia, Res=resuscitation, Reox=30 min after start of reoxygenation, 2h, 5h, 7h=hours after start of reoxygenation.

Paper III. Dynamic FDG-PET for assessing early effects of cerebral hypoxia and resuscitation in new born pigs, Eur J Nucl Med 2012 Feb 2 Epub ahead of print

Purpose

In this paper, we hypothesized that experimental global hypoxia would cause immediate regional changes in glucose metabolism in the brain and that the oxygen content in the resuscitation air would influence the changes. A dynamic FDG-PET method was adapted for quantitative measurement of glucose metabolism by using a microPET system suitable for imaging small animals and newborn babies in clinical practice.

Material and methods

Sixteen piglets were included in this study and subjected to 60 min of hypoxia with FiO_2 0.08 in N_2 and then randomized to 30 min of resuscitation with FiO_2 0.21 (n=8) or FiO_2 1.0 (n=8) followed by 1 h reoxygenation. Dynamic FDG-PET was performed at baseline and then repeated after hypoxia and resuscitation. MRI was performed at the end of the experiment, post-mortem, for anatomic correlation and co-registration with PET. Sagittal 3D TSE T2-weighted images were acquired.

Anesthesia is described in the summary of paper I and in paper II and III. The newborn pigs were anesthetized and tracheotomized. After stabilization, they were transported to the PET examination room nearby where the anesthesia was continued throughout the experiment.

PET scanning was performed in a prone position with the head fixed on the movable table top. Only the head fitted inside the gantry of the scanner. All animals had fasted at least 2 h before the start of the PET examination. A ^{68}Ge source was used for attenuation and scatter correction. 4D dynamic data were reconstructed using OSEM-MAP (2 OSEM iterations, 18 MAP iterations, $\beta = 0.5$, matrix size 128×128×95), providing images with a voxel size of $0.87 \times 0.87 \times 0.80$ mm^3. Total scan time was 50 min. For the baseline study, 20 MBq FDG were administered as a bolus injection by hand in the internal jugular vein. Dynamic PET scanning was started immediately at the end of injection and arterial blood samples (0.3 ml) from the femoral artery were retrieved before start of injection and repeated regularly during scan time. B glucose values were recorded at the start and end of PET scanning.

The second PET study, after hypoxia and resuscitation was performed after the injection of a new dose of 60 MBq.

Analysis of glucose metabolism CMR_{gl} values were estimated from the dynamic FDG-PET series by the Patlak analysis (described in detail in paper III).The slope of the line, *K*, is

proportional to CMR_{gl}. V_0 equals the initial distribution volume (including the fractional blood volume). C_{tissue} was obtained from dynamic FDG-PET and C_p from the arterial blood sampling. LC was chosen to be 0.44. Together with b-glucose values [Glc] of the blood samples, CMR_{gl} was calculated (fig. 9).

MRI and anatomic correlation The 3D MRI images were imported into a software application, for manual delineation of volumes of interest (VOI) in the basal ganglia/ thalamus, the parasagittal cortex bilaterally, white matter, cerebrum and cerebellum. The MR images with VOIs where co-registered with the PET images.

Radiation dose The absorbed organ dose and the effective dose for humans were estimated using the established dose charts from the guidelines of EANM.

Statistical analysis The values of CMR_{gl} in the two resuscitation groups were compared by assessing differences in the regions between baseline and hypoxia/ resuscitation with paired t-test. The same test was performed for the values of volume of distribution V_0. The difference in CMR_{gl} changes between the groups was also compared using Mann-Whitney test.

Results

We found that global hypoxia caused immediate decrease of cerebral glucose metabolism from a mean baseline level (± 1SD) of 21.2± 7.9 to 12.6± 4.7 μmol/min/100 g ($P< 0.01$). The BG, cerebellum, and cortex showed the greatest decrease in CMR_{gl} but no significant differences in global or regional CMR_{gl} between the resuscitation groups were found (table 1).

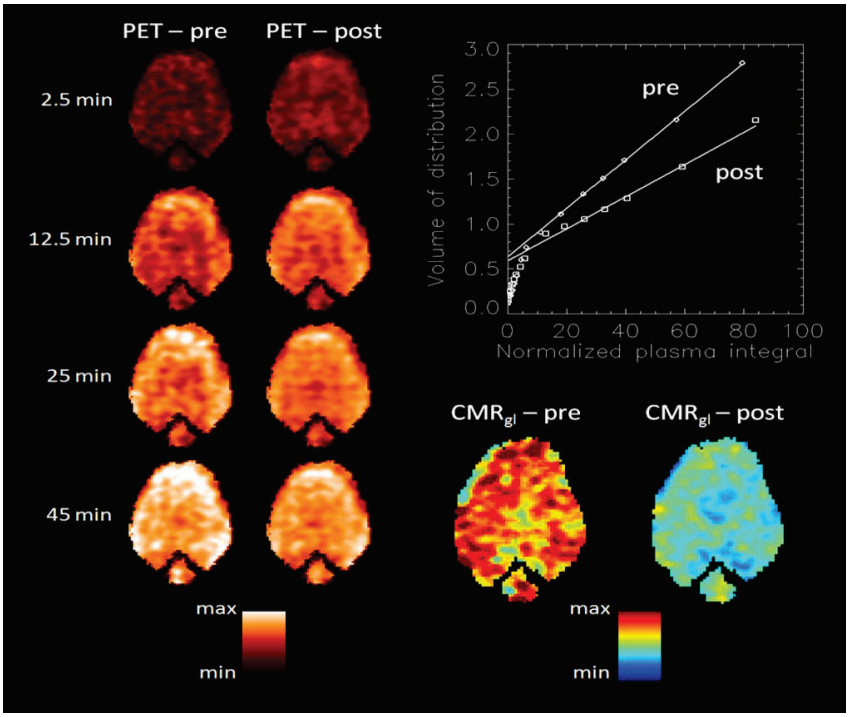

Fig. 9 Parametric maps of increasing tissue activity over time at baseline and after hypoxia and resuscitation (left). Patlak plots for the two time points (top right) and corresponding parametric maps for CMR_{gl} (bottom right). Colour bars indicating max and min FDG tissue activity and CMR_{gl} respectively.

Table 1 CMR_{gl} before and after intervention in the different regions regardless of resuscitation mode.

Region/ VOI	Baseline CMRgl (µmol/min/100g)	After Hypoxia+Res. CMRgl (µmol/min/100g)	After Hypoxia+Res. /Baseline	p-value
Basal ganglia	20.0 (± 8.7)	11.0 (± 4.3)	0.55	.001
Cortex	21.2 (± 5.8)	12.7 (± 4.6)	0.57	.001
Cerebellum	24.6 (± 9.6)	13.6 (± 5.7)	0.55	.003
Cerebrum	20.5 (± 7.8)	12.2 (± 4.6)	0.59	.001
White Matter	20.2 (± 8.4)	12.6 (± 4.7)	0.63	.01

8. Discussion

8.1 The piglet model in MRI investigation of hypoxia-ischemia (Paper I)

In a well-controlled piglet model, HI injury was studied by a correlation between MR findings and histopathological changes.

The recorded reduced ADC and increased Lac correlated strongly to tissue damage, findings in accordance with a retrospective study in newborn infants (54).

ADC values < 0.8 x 10^{-3}/ mm^2/s were found in the basal ganglia in the injured piglets. This is in accordance with clinical findings where these values were shown to always be associated with thalamic infarction (93). We found one piglet without histology proven injury. Piglet's response to hypoxia-ischemia is variable, and preconditioning in intrauterine life may be protective to postnatal injury.

The increased Lac/NAA and Lac/Cho ratios and decreased NAA/Cho and NAA/Cr were in line with previous studies and have been shown to correlate with poor prognosis in clinical studies (53;94). DTI showed increased values in the BG for the piglets as a group 7 h after HI in accordance with an adult study (97). However, three piglets had reduced FA suggesting that FA values are less predictive of injury than ADC.

Animal models will never perfectly mimic the clinical human perinatal situation. The piglets with an age of 12-36 h were already to some extent adapted to extrauterine life. Cerebral maturation is probably quicker in piglets, but piglets and humans are comparable at birth regarding brain growth and myelinization, maturation and distribution of grey to white matter (119). Since our piglets were close to 36 h old at the time of the experiments we do not think this influenced the results significantly.

General anesthesia makes it impossible to observe the animals for neurobehavioral testing. It would be desirable to study the development during the phase of second energy failure, long-term effects, and neurological outcome of the "patients". Such long-term and follow up studies in piglets are difficult, when following the ethical rules and laws of animal research in Norway.

8.2 Cerebral perfusion after hypoxia and resuscitation detected with CEUS and DSC-MRI (Paper II)

This study reports of an early temporal evolution of brain perfusion using CEUS and DSC-MRI in perinatal brain injury in a hypoxic piglet model during and up to 7 h after the insult. These adapted techniques were feasible in the small piglet brain for perfusion quantification.Our main findings were significant regional and general changes in perfusion parameters, indicating increased perfusion during hypoxia followed by a decrease during resuscitation with 100% O_2. In the injured brains (verified by histology) the same changes were found in CEUS (for AUC and PI) and in MRI (for rCBV and MTT). There were only slight but no significant changes over time after normoxic resuscitation. Finally, the perfusion changes were reversible, returning gradually towards baseline values at the endpoint of the experiment, without correlation to histological findings or to decreased diffusion at 7 h. We have studied the cerebrovascular changes over time during the primary energy failure and the early phase of the secondary energy failure. The latter correlates with adverse neurological outcome and depends on the gravity of the first failure (48).

Cerebral hyperperfusion known to occur during hypoxia and early resuscitation could also be demonstrated with CEUS in our study (13). We then found compromised cerebral perfusion with a decrease of PI and AUC during and shortly after resuscitation with 100% of O_2 but not in the normoxic group. This development is probably due to a loss of vascular reactivity caused by the hypoxic event and the fact that hyperoxia causes a reduction of the production of perivascular nitric oxide and an increase of O_2^- with vasoconstriction resulting in reduced cerebral blood flow (44). This decrease in perfusion might be able to cause a more extensive injury evolving during the period of "secondary energy failure".

In this 3T MRI study we were able to measure "low flow" perfusion changes in our hypoxic model. rCBF, which has been shown to be the most important parameter in HI and stroke, did not show significant changes in our study (21;83;91). rCBV changed slightly in accordance with AUC in CEUS, which was also found in a study of brain perfusion in healthy adults (124). Similar to this study, we found AUC the most sensitive parameter to detect hemodynamic changes resulting from hypoxic injury. For the piglets as a group, we found a mismatch between restored perfusion and decreased ADC at 7h.

A fair comparison between CEUS and DSC-MRI is difficult in our study, since we were unable to perform MRI during hypoxia/ resuscitation, where the most significant perfusion

alterations were seen. MRI provides semi-quantitative estimates of perfusion while CEUS provides qualitative perfusion estimates of a 2D scanned sector of the brain.

The anesthetic drugs used in the study may have influenced the CBF. The same combination and dosage of mild continuous anesthesia with midazolam, fentanyl and isoflurane were used for all the animals to ensure minimal distress to the piglets (125). We have tried to minimize and adjust for these influences, in the statistical calculations, by using a control group.

Few clinical studies with CEUS and SonoVue™ have jet been performed in children(62). We did not find injury proven by histology in the control group or in seven of the piglets exposed to hypoxia. During the relatively short time of observation, we did not register any side effects associated to their response to US low energy transmission, even though we injected a double dose of the CA, repeated 8-10 times over 9 h. This is far beyond the recommended doses for adults in clinical practice. The possible damage to the cerebral circulation by trans cranial US has been studied in rats and no adverse effect have been found (58). We speculate that as cerebral US was performed transcranially and with low MI, this may protect brain from the mechanical impact of the US waves to the micro bubbles and to the cerebral tissue.

The use of cyclic non-ionic gadolinium agents like gadobuturol is recommended to minimize the risk of developing a rare but devastating disease, nefrogenic systemic fibrosis (84). These precautions are especially important in neonates due to their immature renal function. The double dose of gadobuturol has been shown to give a better enhancement and was chosen in order to optimize the detection of the low flow perfusion under the experimental study conditions (126).

8.3 Cerebral glucose metabolism after hypoxia and resuscitation detected with FDG-PET (Paper III)

In this study, we established a dynamic FDG-PET method for calculation of CMR_{gl} in the newborn piglet brain using an animal microPET system. The most important results from our study were that global hypoxia caused immediate decrease in cerebral glucose metabolism and that the two modes of resuscitation using normoxia versus hyperoxia, failed to produce a significant difference in the resulting CMR_{gl}. In this very acute phase of

evolving cerebral injury, the glucose hypometabolism may be due to early metabolic down-regulation or early regional cell death.
Previuos animal and human studies have not been able to perform dynamic quantitative measurements of CMR_{gl} (25;29;32;45;111-113). In this study a kinetic analysis of the complete tissue uptake was performed. This in combination with higher resolution in PET images achieved by using the animal microPET system and the use of 3T MRI for VOI delineation, were expected to optimize the detection of the metabolic changes. However, despite these efforts no significant regional difference in cerebral metabolism was found in this early phase after HI, although the most pronounced hypometabolism was found in the deep gray matter, cerebellum and cortex (the most metabolically active regions of the brain).

The interpretation of our findings with hypometabolism is in line with other studies and hypotheses. The combination of hypoxia-ischemia or ischemia alone is necessary for the development of brain injury (14). In our experimental model, the longstanding hypoxia was expected to cause a certain degree of injury although the resulting acid base values indicate that a severe hypoxic injury or anoxia is less likely. Therefore, we assume an early down-regulation of glucose metabolism instead of neuronal death. In a study of the immature rat brain, a decline in CMR_{gl} was found 1 h after hypoxia similar to our findings but was followed by an increase up to 24 h after the insult (31;127). The opposite was discovered after hypoxia-ischemia with a transient increase in CMR_{gl} followed by a decrease. In a study of fetal lambs, marked hypometabolism 4 h after hypoxia ischemia and hyperoxic resuscitation were revealed (45). In these studies however, only autoradiographic calculations of CMR_{gl} were performed, and where quantification in small research animals can be difficult. Human studies measuring SUV and relative values of CMR_{gl} have shown regional hyper- and hypometabolism a few days after birth correlating well with neurological outcome (32;113). Our short-term results do not allow prediction of outcome but may indicate the possibility of a later development of hypermetabolism according to these human and animal studies. Hypermetabolism that may be associated with less severe neurological outcome. Still long-term studies reaching beyond the period of second energy failure would be necessary to reveal these possible changes and outcomes.

The correction term, LC is assumed constant in the normal brain. Under pathological conditions changes in LC occur and may increase several times in ischemic regions of the brain (116). The value of LC in the normal newborn brain is not known. The chosen LC of

0.44 for our study represents a limitation, in that the posthypoxic estimate of CMR_{gl} may be underestimated under hypometabolism due to an expected increase in LC. To establish the true LC uptake of 3-0-[^{11}C] methyl-D-glucose must be performed in the future, since this tracer was unavailable at the time of our study.

8.4 General discussion

Birth asphyxia is an important worldwide problem with major morbidity and mortality factors (1;9;47). The primary goals of management of a newborn asphyctic baby are early identification of the baby at highest risk for developing injury and consideration of intervention. Assessment of cerebral injury can help to predict outcome of the HIE, which remains a major marker of perinatal morbidity and neurodevelopmental disabilities (53).

Animal research models play an important role when studying the pathophysiology of the very early phase in perinatal HI injury. These pathophysiological mechanisms in particular of cerebral perfusion and glucose metabolism, are the key to the further development of HIE. Finding and developing neuroimaging and biochemical tools to investigate HI mechanisms in the early phase after the insult are important for initiating early neuroprotective treatment.

Our hypoxic ischemic piglet model has similarities with a newborn baby in the perinatal HI situation. The model can produce histopathologic findings of HI injury in accordance with findings on MRI/ MRS 7 h after the insult, which again is in line with findings in clinical studies (93). This piglet model has helped to establish diagnostic methods in MRI, US and PET, adapted to detect early effects of cerebral perinatal hypoxia with regard to perfusion, diffusion, and glucose metabolism in the early post hypoxic period.

Our main findings were an early temporal development of brain perfusion measured by CEUS and DSC-MRI in perinatal hypoxic piglet model during and up to 7 h after the insult. Low flow perfusion quantification was feasible in the small piglet brain. We found a mismatch between restored perfusion and diffusion at the end of the experiment without correlation to histological findings suggesting viable, penumbral tissue (82;83). CEUS used during hypoxia and resuscitation could demonstrate the most important perfusion changes in accordance with other animal studies using other techniques (13;17;44).

CEUS, is a technique with higher temporal resolution than DSC-MRI and can demonstrate perfusion in real time (60). CEUS and the CA SonoVue™ is not jet registered for pediatric use. Our experience showed that transcranial CEUS was safe in newborn piglets.

Ventilation with high-level concentration of oxygen has proven harmful to the brain and other organs (38-41;121). Resuscitation with air is now recommended for term and near term infants by ILCOR (42). The toxic mechanisms of hyperoxia to different organs are not fully understood or studied, especially regarding cerebrovascular and metabolic changes in HIE. CEUS revealed that oxidative stress caused a cerebral hypoperfusion, probably due to vasoconstriction as confirmed by a study in rats (44). This decrease in perfusion might cause a more extensive injury developing during the period of "secondary energy failure".
Dynamic FDG-PET revealed marked hypometabolism of glucose after prolonged global hypoxia as found in other animal studies (31;127). In this very acute phase of evolving cerebral injury, the glucose hypometabolism may be due to early metabolic down regulation or early regional cell death. No significant change related to hyperoxia was found. Earlier animal and human newborn studies have not been able to perform dynamic quantitative measurements of CMR_{gl} (28;29;31;32;45;111-113;127). In clinical studies, relative glucose values or semiquantitative measurements have been performed a few days after birth. They revealed hyper- and hypometabolism as associated with short-term neurological outcome (25;112;113).The adapted techniques, CEUS, DSC-MRI and dynamic FDG-PET have been shown to be feasible in the newborn piglet brain under experimental HI conditions.

9. Conclusions and future aspects

9.1 Conclusions

1. Our piglet model is suitable for investigating HI injury with neuroimaging techniques, MRI and MRS, and may be relevant to the clinical perinatal situation.

2. Quantification of cerebral perfusion with CEUS and DSC-MRI in addition to glucose metabolism with dynamic FDG PET is feasible in the newborn piglet brain.

3. Our perinatal hypoxia model revealed an evolution of perfusion changes over time with restored values after 7 h, without significant correlation to histological injury or to decreased diffusion. The results suggest that CEUS/ DSC-MRI cannot be used alone in the early diagnosis of perinatal hypoxia

4. Dynamic FDG-PET can assess early effects of cerebral perinatal hypoxia. In the piglet model, global hypoxia caused immediate decrease of cerebral glucose metabolism.

5. Hyperoxic (100% O_2) resuscitation causes immediate decreased cerebral perfusion not seen when normoxia (21 % O_2) is used. No significant effect of hyperoxia was found on glucose metabolism.

9.2 Future aspects

By using a piglet model resembling a newborn baby, our experimental studies may contribute to the further understanding of perinatal hypoxia injury mechanisms and regulation of cerebral perfusion. We indicate a potential use of CEUS to monitor, in real time, cerebral perfusion changes during different treatment strategies aiming to prevent cerebral injury under experimental conditions. The absence of radiation combined with the easy bedside use of CEUS, makes this technique attractive for pediatric use, especially in critically ill infants. However, further clinical studies are needed. By the introduction of MR compatible incubators, the monitoring of vulnerable term and premature babies during transport and examination will facilitate MR studies at an earlier time point after birth.The technical development of non-contrast enhanced perfusion techniques like ASL will likely

become more important in pediatric imaging, especially in the light of increasing concerns about the toxic effects of gadolinium and expensive CAs.

Further studies of FDG-PET, reaching beyond the period of secondary energy failure and studies to establish the LC in newborn hypoxic piglets, are needed to get more accurate quantification of the CMR_{gl}. MicroPET systems might be a useful clinical easy-access tool to evaluate brain function in newborn babies and be important in diagnosis and prognosis of perinatal hypoxia. Multiple tracers, receptor ligands or hypoxia markers applicable in PET combined with MRI in hybrid scanners, will be able to provide us with further understanding of cerebral perinatal HI injury.

Reference List

(1) Azra HB, Bhutta ZA. Birth asphyxia in developing countries: current status and public health implications. Curr Probl Pediatr Adolesc Health Care 2006 May;36(5):178-88.

(2) Black RE, Cousens S, Johnson HL, Lawn JE, Rudan I, Bassani DG, et al. Global, regional, and national causes of child mortality in 2008: a systematic analysis. Lancet 2010 Jun 5;375(9730):1969-87.

(3) Mwaniki MK, Atieno M, Lawn JE, Newton CR. Long-term neurodevelopmental outcomes after intrauterine and neonatal insults: a systematic review. Lancet 2012 Feb 4;379(9814)445-52.

(4) Ferriero DM. Neonatal brain injury. N Engl J Med 2004 Nov 4;351(19):1985-95.

(5) Lawn JE, Bahl R, Bergstrom S, Bhutta ZA, Darmstadt GL, Ellis M, et al. Setting research priorities to reduce almost one million deaths from birth asphyxia by 2015. PLoS Med 2011;8(1):e1000389.

(6) ACOG Committee Opinion #303: Inappropriate use of the terms fetal distress and birth asphyxia. Obstet Gynecol 2004 Oct;104(4):903.

(7) Nelson KB, Leviton A. How much of neonatal encephalopathy is due to birth asphyxia? Am J Dis Child 1991 Nov;145(11):1325-31.

(8) Perlman JM. Summary proceedings from the neurology group on hypoxic-ischemic encephalopathy. Pediatrics 2006 Mar;117(3 Pt 2):S28-S33.

(9) Fatemi A, Wilson MA, Johnston MV. Hypoxic-ischemic encephalopathy in the term infant. Clin Perinatol 2009 Dec;36(4):835-58, vii.

(10) Lorek A, Takei Y, Cady EB, Wyatt JS, Penrice J, Edwards AD, et al. Delayed ("secondary") cerebral energy failure after acute hypoxia-ischemia in the newborn piglet: continuous 48-hour studies by phosphorus magnetic resonance spectroscopy. Pediatr Res 1994 Dec;36(6):699-706.

(11) Gluckman PD, Williams CE. When and why do brain cells die? Dev Med Child Neurol 1992 Nov;34(11):1010-4.

(12) Shalak L, Perlman JM. Hypoxic-ischemic brain injury in the term infant-current concepts. Early Hum Dev 2004 Nov;80(2):125-41.

(13) Berger R, Garnier Y. Perinatal brain injury. J Perinat Med 2000;28(4):261-85.

(14) Johnston MV, Trescher WH, Ishida A, Nakajima W. Neurobiology of hypoxic-ischemic injury in the developing brain. Pediatr Res 2001 Jun;49(6):735-41.

(15) Vannucci RC. Experimental biology of cerebral hypoxia-ischemia: relation to perinatal brain damage. Pediatr Res 1990 Apr;27(4 Pt 1):317-26.

(16) Solas AB, Kalous P, Saugstad OD. Reoxygenation with 100 or 21% oxygen after cerebral hypoxemia-ischemia-hypercapnia in newborn piglets. Biol Neonate 2004;85(2):105-11.

(17) Rosenberg AA, Murdaugh E, White CW. The role of oxygen free radicals in postasphyxia cerebral hypoperfusion in newborn lambs. Pediatr Res 1989 Sep;26(3):215-9.

(18) Pryds O, Greisen G, Lou H, Friis-Hansen B. Vasoparalysis associated with brain damage in asphyxiated term infants. J Pediatr 1990 Jul;117(1 Pt 1):119-25.

(19) Heiss WD. Ischemic penumbra: evidence from functional imaging in man. J Cereb Blood Flow Metab 2000 Sep;20(9):1276-93.

(20) Marin T, Moore J. Understanding near-infrared spectroscopy. Adv Neonatal Care 2011 Dec;11(6):382-8.

(21) Goff DA, Buckley EM, Durduran T, Wang J, Licht DJ. Noninvasive cerebral perfusion imaging in high-risk neonates. Semin Perinatol 2010 Feb;34(1):46-56.

(22) Ilves P, Lintrop M, Metsvaht T, Vaher U, Talvik T. Cerebral blood-flow velocities in predicting outcome of asphyxiated newborn infants. Acta Paediatrica 2004 Apr;93(4):523-8.

(23) Prinzen FW, Bassingthwaighte JB. Blood flow distributions by microsphere deposition methods. Cardiovasc Res 2000 Jan 1;45(1):13-21.

(24) Shi Y, Jin RB, Zhao JN, Tang SF, Li HQ, Li TY. Brain positron emission tomography in preterm and term newborn infants. Early Hum Dev 2009 Jul;85(7):429-32.

(25) Thorngren-Jerneck K, Ohlsson T, Sandell A, Erlandsson K, Strand SE, Ryding E, et al. Cerebral glucose metabolism measured by positron emission tomography in term newborn infants with hypoxic ischemic encephalopathy. Pediatr Res 2001 Apr;49(4):495-501.

(26) Choi DW, Rothman SM. The role of glutamate neurotoxicity in hypoxic-ischemic neuronal death. Annu Rev Neurosci 1990;13:171-82.

(27) Chugani HT, Phelps ME, Mazziotta JC. Positron emission tomography study of human brain functional development. Ann Neurol 1987 Oct;22(4):487-97.

(28) Shi Y, Zhao JN, Liu L, Hu ZX, Tang SF, Chen L, et al. Changes of positron emission tomography in newborn infants at different gestational ages, and neonatal hypoxic-ischemic encephalopathy. Pediatr Neurol 2012 Feb;46(2):116-23.

(29) Vannucci RC, Christensen MA, Stein DT. Regional cerebral glucose utilization in the immature rat: effect of hypoxia-ischemia. Pediatr Res 1989 Sep;26(3):208-14.

(30) Ginsberg MD, Graham DI, Busto R. Regional glucose utilization and blood flow following graded forebrain ischemia in the rat: correlation with neuropathology. Ann Neurol 1985 Oct;18(4):470-81.

(31) Vannucci RC, Yager JY, Vannucci SJ. Cerebral glucose and energy utilization during the evolution of hypoxic-ischemic brain damage in the immature rat. J Cereb Blood Flow Metab 1994 Mar;14(2):279-88.

(32) Blennow M, Ingvar M, Lagercrantz H, Stone-Elander S, Eriksson L, Forssberg H, et al. Early [18F]FDG positron emission tomography in infants with hypoxic-ischaemic encephalopathy shows hypermetabolism during the postasphyctic period. Acta Paediatr 1995 Nov;84(11):1289-95.

(33) Heiss WD, Herholz K. Assessment of pathophysiology of stroke by positron emission tomography. Eur J Nucl Med 1994 May;21(5):455-65.

(34) Chao CP, Zaleski CG, Patton AC. Neonatal hypoxic-ischemic encephalopathy: multimodality imaging findings. Radiographics 2006 Oct;26 Suppl 1:S159-S172.

(35) Rutherford M, Biarge MM, Allsop J, Counsell S, Cowan F. MRI of perinatal brain injury. Pediatr Radiol 2010 Jun;40(6):819-33.

(36) Obladen M. History of neonatal resuscitation. Part 2: oxygen and other drugs. Neonatology 2009;95(1):91-6.

(37) Saugstad OD, Aasen AO. Plasma hypoxanthine concentrations in pigs. A prognostic aid in hypoxia. Eur Surg Res 1980;12(2):123-9.

(38) Munkeby BH, Borke WB, Bjornland K, Sikkeland LI, Borge GI, Lomo J, et al. Resuscitation of hypoxic piglets with 100% o2 increases pulmonary metalloproteinases and IL-8. Pediatr Res 2005 Sep;58(3):542-8.

(39) Saugstad OD, Ramji S, Soll RF, Vento M. Resuscitation of Newborn Infants with 21% or 100% Oxygen: An Updated Systematic Review and Meta-Analysis. Neonatology 2008 Jul 9;94(3):176-82.

(40) Saugstad OD. Is oxygen more toxic than currently believed? Pediatrics 2001 Nov;108(5):1203-5.

(41) Vento M, Sastre J, Asensi MA, Vina J. Room-air resuscitation causes less damage to heart and kidney than 100% oxygen. Am J Respir Crit Care Med 2005 Dec 1;172(11):1393-8.

(42) Biban P, Filipovic-Grcic B, Biarent D, Manzoni P. New cardiopulmonary resuscitation guidelines 2010: managing the newly born in delivery room. Early Hum Dev 2011 Mar;87 Suppl 1:S9-11.

(43) Lundstrom KE, Pryds O, Greisen G. Oxygen at birth and prolonged cerebral vasoconstriction in preterm infants. Arch Dis Child Fetal Neonatal Ed 1995 Sep;73(2):F81-F86.

(44) Fabian RH, Perez-Polo JR, Kent TA. Perivascular nitric oxide and superoxide in neonatal cerebral hypoxia-ischemia. Am J Physiol Heart Circ Physiol 2008 Oct;295(4):H1809-H1814.

(45) Thorngren-Jerneck K, Ley D, Hellstrom-Westas L, Hernandez-Andrade E, Lingman G, Ohlsson T, et al. Reduced postnatal cerebral glucose metabolism measured by PET after asphyxia in near term fetal lambs. J Neurosci Res 2001 Dec 1;66(5):844-50.

(46) Sarnat HB, Sarnat MS. Neonatal encephalopathy following fetal distress. A clinical and electroencephalographic study. Arch Neurol 1976 Oct;33(10):696-705.

(47) Accardo J, Kammann H, Hoon Jr AH. Neuroimaging in cerebral palsy. The Journal of Pediatrics 2004 Aug;145(2, Supplement 1):S19-S27.

(48) Cotten CM, Shankaran S. Hypothermia for hypoxic-ischemic encephalopathy. Expert Rev Obstet Gynecol 2010 Mar 1;5(2):227-39.

(49) Pfister RH, Soll RF. Hypothermia for the treatment of infants with hypoxic-ischemic encephalopathy. J Perinatol 2010 Oct;30 Suppl:S82-S87.

(50) Azzopardi DV, Strohm B, Edwards AD, Dyet L, Halliday HL, Juszczak E, et al. Moderate hypothermia to treat perinatal asphyxial encephalopathy. N Engl J Med 2009 Oct 1;361(14):1349-58.

(51) Gluckman PD, Wyatt JS, Azzopardi D, Ballard R, Edwards AD, Ferriero DM, et al. Selective head cooling with mild systemic hypothermia after neonatal encephalopathy: multicentre randomised trial. Lancet 2005 Feb 19;365(9460):663-70.

(52) Edwards AD, Brocklehurst P, Gunn AJ, Halliday H, Juszczak E, Levene M, et al. Neurological outcomes at 18 months of age after moderate hypothermia for perinatal hypoxic ischaemic encephalopathy: synthesis and meta-analysis of trial data. BMJ 2010 Feb;9:340:c363.

(53) Barkovich AJ, Baranski K, Vigneron D, Partridge JC, Hallam DK, Hajnal BL, et al. Proton MR spectroscopy for the evaluation of brain injury in asphyxiated, term neonates. AJNR Am J Neuroradiol 1999 Sep;20(8):1399-405.

(54) Boichot C, Walker PM, Durand C, Grimaldi M, Chapuis S, Gouyon JB, et al. Term neonate prognoses after perinatal asphyxia: contributions of MR imaging, MR spectroscopy, relaxation times, and apparent diffusion coefficients. Radiology 2006 Jun;239(3):839-48.

(55) Liauw L, van der Grond J, van den Berg-Huysmans AA, Palm-Meinders IH, van Buchem MA, van Wezel-Meijler G. Hypoxic-ischemic encephalopathy: diagnostic value of conventional MR imaging pulse sequences in term-born neonates. Radiology 2008 Apr;247(1):204-12.

(56) Kannan S, Chugani HT. Applications of positron emission tomography in the newborn nursery. Semin Perinatol 2010 Feb;34(1):39-45.

(57) Munkeby BH, Lyng K, Froen JF, Winther-Larssen EH, Rosland JH, Smith HJ, et al. Morphological and hemodynamic magnetic resonance assessment of early neonatal brain injury in a piglet model. J Magn Reson Imaging 2004 Jul;20(1):8-15.

(58) Haggag KJ, Russell D, Walday P, Skiphamn A, Torvik A. Air-filled ultrasound contrast agents do not damage the cerebral microvasculature or brain tissue in rats. Invest Radiol 1998 Mar;33(3):129-35.

(59) Greis C. Technology overview: sonoVue. European Radiology Supplements 2004 Oct;14(0):11-5.

(60) Lim A, Cosgrove D. Functional studies. European Radiology Supplements 2004 Oct;14(0):110-5.

(61) Schneider M. SonoVue, a new ultrasound contrast agent. Eur Radiol 1999;9 Suppl 3:S347-S348.

(62) Valentino M, Serra C, Pavlica P, Labate AM, Lima M, Baroncini S, et al. Blunt abdominal trauma: diagnostic performance of contrast-enhanced US in children--initial experience. Radiology 2008 Mar;246(3):903-9.

(63) Geleijnse ML, Nemes A, Vletter WB, Michels M, Soliman OI, Caliskan K, et al. Adverse reactions after the use of sulphur hexafluoride (SonoVue) echo contrast agent. J Cardiovasc Med (Hagerstown) 2009 Jan;10(1):75-7.

(64) Bartels E, Bittermann HJ. Transcranial contrast imaging of cerebral perfusion in stroke patients following decompressive craniectomy. Ultraschall Med 2004 Jun;25(3):206-13.

(65) Kern R, Perren F, Schoeneberger K, Gass A, Hennerici M, Meairs S. Ultrasound Microbubble Destruction Imaging in Acute Middle Cerebral Artery Stroke. Stroke 2004 Jul 1;35(7):1665-70.

(66) Seidel G, Cangur H, Meyer-Wiethe K, Renault G, Herment A, Schindler A, et al. On the ability of ultrasound parametric perfusion imaging to predict the area of infarction in acute ischemic stroke. Ultraschall Med 2006 Dec;27(6):543-8.

(67) Flores R, Hennings LJ, Lowery JD, Brown AT, Culp WC. Microbubble-Augmented Ultrasound Sonothrombolysis Decreases Intracranial Hemorrhage in a Rabbit Model of Acute Ischemic Stroke. Invest Radiol 2011 Jul;46(7):419-24

(68) Seidel G, Algermissen C, Christoph A, Katzer T, Kaps M, Baumgartner RW. Visualization of Brain Perfusion With Harmonic Gray Scale and Power Doppler Technology : An Animal Pilot Study Editorial Comment: An Animal Pilot Study. Stroke 2000 Jul 1;31(7):1728-34.

(69) van Wijk MC, Klaessens JH, Hopman JC, Liem KD, Thijssen JM. Assessment of local changes of cerebral perfusion and blood concentration by ultrasound harmonic B-mode contrast measurement in piglet. Ultrasound Med Biol 2003 Sep;29(9):1253-60.

(70) Hendee WR, Morgan CJ. Magnetic resonance imaging. Part I--physical principles. West J Med 1984 Oct;141(4):491-500.

(71) Rutherford M, Srinivasan L, Dyet L, Ward P, Allsop J, Counsell S, et al. Magnetic resonance imaging in perinatal brain injury: clinical presentation, lesions and outcome. Pediatr Radiol 2006 Jul;36(7):582-92.

(72) Triulzi F, Parazzini C, Righini A. Patterns of damage in the mature neonatal brain. Pediatr Radiol 2006 Jul;36(7):608-20.

(73) Barkovich AJ, Westmark K, Partridge C, Sola A, Ferriero DM. Perinatal asphyxia: MR findings in the first 10 days. AJNR Am J Neuroradiol 1995 Mar;16(3):427-38.

(74) Barbier EL, Lamalle L, Decorps M. Methodology of brain perfusion imaging. J Magn Reson Imaging 2001 Apr;13(4):496-520.

(75) Chen J, Licht DJ, Smith SE, Agner SC, Mason S, Wang S, et al. Arterial spin labeling perfusion MRI in pediatric arterial ischemic stroke: initial experiences. J Magn Reson Imaging 2009 Feb;29(2):282-90.

(76) Detre JA, Rao H, Wang DJ, Chen YF, Wang Z. Applications of arterial spin labeled MRI in the brain. J Magn Reson Imaging 2012 May;35(5):1026-37.

(77) Huisman TA, Sorensen AG. Perfusion-weighted magnetic resonance imaging of the brain: techniques and application in children. Eur Radiol 2004 Jan;14(1):59-72.

(78) Ostergaard L, Weisskoff RM, Chesler DA, Gyldensted C, Rosen BR. High resolution measurement of cerebral blood flow using intravascular tracer bolus passages. Part I: Mathematical approach and statistical analysis. Magn Reson Med 1996 Nov;36(5):715-25.

(79) Wu O, Ostergaard L, Weisskoff RM, Benner T, Rosen BR, Sorensen AG. Tracer arrival timing-insensitive technique for estimating flow in MR perfusion-weighted imaging using singular value decomposition with a block-circulant deconvolution matrix. Magn Reson Med 2003 Jul;50(1):164-74.

(80) Laswad T, Wintermark P, Alamo L, Moessinger A, Meuli R, Gudinchet F. Method for performing cerebral perfusion-weighted MRI in neonates. Pediatr Radiol 2009 Mar;39(3):260-4.

(81) Westmark KD, Barkovich AJ, Sola A, Ferriero D, Partridge JC. Patterns and implications of MR contrast enhancement in perinatal asphyxia: a preliminary report. Ajnr: American Journal of Neuroradiology 1995 Apr;16(4):685-92.

(82) Wintermark P, Moessinger AC, Gudinchet F, Meuli R. Perfusion-weighted magnetic resonance imaging patterns of hypoxic-ischemic encephalopathy in term neonates. J Magn Reson Imaging 2008 Oct;28(4):1019-25.

(83) Wintermark P, Moessinger AC, Gudinchet F, Meuli R. Temporal evolution of MR perfusion in neonatal hypoxic-ischemic encephalopathy. J Magn Reson Imaging 2008 Jun;27(6):1229-34.

(84) Mendichovszky IA, Marks SD, Simcock CM, Olsen OE. Gadolinium and nephrogenic systemic fibrosis: time to tighten practice. Pediatr Radiol 2008 May;38(5):489-96.

(85) Wintermark P, Hansen A, Gregas MC, Soul J, Labrecque M, Robertson RL, et al. Brain perfusion in asphyxiated newborns treated with therapeutic hypothermia. AJNR Am J Neuroradiol 2011 Dec;32(11):2023-9.

(86) Hagmann P, Jonasson L, Maeder P, Thiran JP, Wedeen VJ, Meuli R. Understanding diffusion MR imaging techniques: from scalar diffusion-weighted imaging to diffusion tensor imaging and beyond. Radiographics 2006 Oct;26 Suppl 1:S205-S223.

(87) Rennie J, Hagman C, Robertson N. Neonatal cerebral investigation. 32-34. 2008.
Ref Type: Generic

(88) Moseley ME, Cohen Y, Mintorovitch J, Chileuitt L, Shimizu H, Kucharczyk J, et al. Early detection of regional cerebral ischemia in cats: comparison of diffusion- and T2-weighted MRI and spectroscopy. Magn Reson Med 1990 May;14(2):330-46.

(89) Burgess RE, Kidwell CS. Use of MRI in the assessment of patients with stroke. Curr Neurol Neurosci Rep 2011 Feb;11(1):28-34.

(90) Donnan GA, Davis SM. Neuroimaging, the ischaemic penumbra, and selection of patients for acute stroke therapy. Lancet Neurol 2002 Nov;1(7):417-25.

(91) Schaefer PW, Ozsunar Y, He J, Hamberg LM, Hunter GJ, Sorensen AG, et al. Assessing tissue viability with MR diffusion and perfusion imaging. AJNR Am J Neuroradiol 2003 Mar;24(3):436-43.

(92) Robertson RL, Ben-Sira L, Barnes PD, Mulkern RV, Robson CD, Maier SE, et al. MR line-scan diffusion-weighted imaging of term neonates with perinatal brain ischemia. AJNR Am J Neuroradiol 1999 Oct;20(9):1658-70.

(93) Rutherford M, Counsell S, Allsop J, Boardman J, Kapellou O, Larkman D, et al. Diffusion-weighted magnetic resonance imaging in term perinatal brain injury: a comparison with site of lesion and time from birth. Pediatrics 2004 Oct;114(4):1004-14.

(94) Alderliesten T, de Vries LS, Benders MJ, Koopman C, Groenendaal F. MR imaging and outcome of term neonates with perinatal asphyxia: value of diffusion-weighted MR imaging and (1)H MR spectroscopy. Radiology 2011 Oct;261(1):235-42.

(95) Dubois J, Dehaene-Lambertz G, Mangin JF, Le BD, Huppi PS, Hertz-Pannier L. [Brain development of infant and MRI by diffusion tensor imaging]. Neurophysiol Clin 2012 Jan;42(1-2):1-9.

(96) Huppi PS, Murphy B, Maier SE, Zientara GP, Inder TE, Barnes PD, et al. Microstructural brain development after perinatal cerebral white matter injury assessed by diffusion tensor magnetic resonance imaging. Pediatrics 2001 Mar;107(3):455-60.

(97) Ozsunar Y, Grant PE, Huisman TA, Schaefer PW, Wu O, Sorensen AG, et al. Evolution of water diffusion and anisotropy in hyperacute stroke: significant correlation between fractional anisotropy and T2. AJNR Am J Neuroradiol 2004 May;25(5):699-705.

(98) Porter EJ, Counsell SJ, Edwards AD, Allsop J, Azzopardi D. Tract-based spatial statistics of magnetic resonance images to assess disease and treatment effects in perinatal asphyxial encephalopathy. Pediatr Res 2010 Sep;68(3):205-9.

(99) Rennie J, Hagman C, Robertson NJ. Neonatal cerebral investigation. 35-39. 2008.
Ref Type: Generic

(100) Huppi PS, Lazeyras F. Proton magnetic resonance spectroscopy ((1)H-MRS) in neonatal brain injury. Pediatr Res 2001 Mar;49(3):317-20.

(101) Barkovich AJ, Westmark KD, Bedi HS, Partridge JC, Ferriero DM, Vigneron DB. Proton spectroscopy and diffusion imaging on the first day of life after perinatal asphyxia: preliminary report. AJNR Am J Neuroradiol 2001 Oct;22(9):1786-94.

(102) Zarifi MK, Astrakas LG, Poussaint TY, Plessis AA, Zurakowski D, Tzika AA. Prediction of adverse outcome with cerebral lactate level and apparent diffusion coefficient in infants with perinatal asphyxia. Radiology 2002 Dec;225(3):859-70.

(103) Cappellini M, Rapisardi G, Cioni ML, Fonda C. Acute hypoxic encephalopathy in the full-term newborn: correlation between Magnetic Resonance Spectroscopy and neurological evaluation at short and long term. Radiol Med 2002 Oct;104(4):332-40.

(104) Cady EB. Metabolite concentrations and relaxation in perinatal cerebral hypoxic-ischemic injury. Neurochem Res 1996 Sep;21(9):1043-52.

(105) Alger JR. Quantitative proton magnetic resonance spectroscopy and spectroscopic imaging of the brain: a didactic review. Top Magn Reson Imaging 2010 Apr;21(2):115-28.

(106) Sokoloff L, Reivich M, Kennedy C, Des Rosiers MH, Patlak CS, Pettigrew KD, et al. The [14C]deoxyglucose method for the measurement of local cerebral glucose utilization: theory, procedure, and normal values in the conscious and anesthetized albino rat. J Neurochem 1977 May;28(5):897-916.

(107) Thorp PS, Levin SD, Garnett ES, Nahmias C, Firnau G, Toi A, et al. Patterns of cerebral glucose metabolism using 18FDG and positron tomography in the neurologic investigation of the full term newborn infant. Neuropediatrics 1988 Aug;19(3):146-53.

(108) Heiss WD, Emunds HG, Herholz K. Cerebral glucose metabolism as a predictor of rehabilitation after ischemic stroke. Stroke 1993 Dec;24(12):1784-8.

(109) Stauss J, Franzius C, Pfluger T, Juergens KU, Biassoni L, Begent J, et al. Guidelines for 18F-FDG PET and PET-CT imaging in paediatric oncology. Eur J Nucl Med Mol Imaging 2008 Aug;35(8):1581-8.

(110) Shrimpton PC, Hillier MC, Lewis MA, Dunn M. National survey of doses from CT in the UK: 2003. Br J Radiol 2006 Dec;79(948):968-80.

(111) Batista CE, Chugani HT, Juhasz C, Behen ME, Shankaran S. Transient hypermetabolism of the basal ganglia following perinatal hypoxia. Pediatr Neurol 2007 May;36(5):330-3.

(112) Doyle LW, Nahmias C, Firnau G, Kenyon DB, Garnett ES, Sinclair JC. Regional cerebral glucose metabolism of newborn infants measured by positron emission tomography. Dev Med Child Neurol 1983 Apr;25(2):143-51.

(113) Suhonen-Polvi H, Kero P, Korvenranta H, Ruotsalainen U, Haaparanta M, Bergman J, et al. Repeated fluorodeoxyglucose positron emission tomography of the brain in infants with suspected hypoxic-ischaemic brain injury. Eur J Nucl Med 1993 Sep;20(9):759-65.

(114) Thorngren-Jerneck K, Hellstrom-Westas L, Ryding E, Rosen I. Cerebral glucose metabolism and early EEG/aEEG in term newborn infants with hypoxic-ischemic encephalopathy. Pediatr Res 2003 Dec;54(6):854-60.

(115) Patlak CS, Blasberg RG. Graphical evaluation of blood-to-brain transfer constants from multiple-time uptake data. Generalizations. J Cereb Blood Flow Metab 1985 Dec;5(4):584-90.

(116) Gjedde A, Wienhard K, Heiss WD, Kloster G, Diemer NH, Herholz K, et al. Comparative regional analysis of 2-fluorodeoxyglucose and methylglucose uptake in brain of four stroke patients. With special reference to the regional estimation of the lumped constant. J Cereb Blood Flow Metab 1985 Jun;5(2):163-78.

(117) Wintermark M, Sesay M, Barbier E, Borbely K, Dillon WP, Eastwood JD, et al. Comparative overview of brain perfusion imaging techniques. J Neuroradiol 2005 Dec;32(5):294-314.

(118) Wechsler LR. Imaging evaluation of acute ischemic stroke. Stroke 2011 Jan;42(1 Suppl):S12-S15.

(119) Grate LL, Golden JA, Hoopes PJ, Hunter JV, Duhaime AC. Traumatic brain injury in piglets of different ages: techniques for lesion analysis using histology and magnetic resonance imaging. J Neurosci Methods 2003 Mar 15;123(2):201-6.

(120) Rice JE, III, Vannucci RC, Brierley JB. The influence of immaturity on hypoxic-ischemic brain damage in the rat. Ann Neurol 1981 Feb;9(2):131-41.

(121) Munkeby BH., Borke WB., Bjornland K., Sikkeland LIB., Borge GIA., Halvorsen B., et al. Resuscitation with 100% O2 Increases Cerebral Injury in Hypoxemic Piglets. Pediatr Res 2004 Nov 1;56(5):783-90.

(122) Rootwelt T, Loberg EM, Moen A, Oyasaeter S, Saugstad OD. Hypoxemia and reoxygenation with 21% or 100% oxygen in newborn pigs: changes in blood pressure, base deficit, and hypoxanthine and brain morphology. Pediatr Res 1992 Jul;32(1):107-13.

(123) Foster KA, Colditz PB, Lingwood BE, Burke C, Dunster KR, Roberts MS. An improved survival model of hypoxia/ischaemia in the piglet suitable for neuroprotection studies. Brain Res 2001 Nov 16;919(1):122-31.

(124) Harrer JU, Klotzsch C, Stracke CP, Moller-Hartmann W. [Cerebral perfusion sonography in comparison with perfusion MRT: a study with healthy volunteers]. Ultraschall Med 2004 Aug;25(4):263-9.

(125) Smith AC, Zellner JL, Spinale FG, Swindle MM. Sedative and cardiovascular effects of midazolam in swine. Lab Anim Sci 1991 Apr;41(2):157-61.

(126) Essig M, Lodemann KP, Le-Huu M, Bruning R, Kirchin M, Reith W. Intraindividual comparison of gadobenate dimeglumine and gadobutrol for cerebral magnetic resonance perfusion imaging at 1.5 T. Invest Radiol 2006 Mar;41(3):256-63.

(127) Gilland E, Bona E, Hagberg H. Temporal changes of regional glucose use, blood flow, and microtubule-associated protein 2 immunostaining after hypoxia-ischemia in the immature rat brain. J Cereb Blood Flow Metab 1998 Feb;18(2):222-8.

PAPER I-III

I

II

III

Errata Paper I

A few references were regrettably erroneously cited due to problems in the publication process.

-In Material and Methods

/ Magnetic resonance imaging/ line 4: reference (15) should be omitted.

/ Image analysis/ second paragraph/ line 5: reference (14) should be changed to reference (9)./ Evaluation (immunohistochemistry)/ line 4 for from end of paragraph: reference (16) should be omitted and replaced by: *Johnson GV, Jope RS. The role of microtubule-associated protein 2 (MAP-2)in neuronal growth, plasticity, and degeneration. J Neurosci Res 1992;33(4):505-512*.

-In Discussion

/ paragraph 3 from the end of section/ line 4: reference (40) should be omitted and changed to reference (21).

/ paragraph 3 from the end of section / line 5 – reference (21) should be replaced by:

Cady EB. Metabolite concentrations and relaxation in perinatal cerebral hypoxic–ischaemic injury. Neurochem Res 1996; 21: 1043–52.

Errata for:

Early effects of perinatal hypoxia and resuscitation on cerebral perfusion and metabolism assessed by MRI, CEUS and FDG-PET.
Experimental studies in newborn pigs.

Page 12, Last paragraph/ first sentence:
"HI" should be changed to "hypoxia ischemia"

Page 48, Second paragraph, second line:
After "HI" - "injury" should be inserted.

References:

Corrected and updated publication dates to:

(3) Mwaniki MK, Atieno M, Lawn JE, Newton CR. Long-term neurodevelopmental outcomes after intrauterine and neonatal insults: a systematic review. Lancet 2012 Feb 4;379(9814)445-52.

(22) Ilves P, Lintrop M, Metsvaht T, Vaher U, Talvik T. Cerebral blood-flow velocities in predicting outcome of asphyxiated newborn infants. Acta Paediatrica 2004 Apr;93(4):523-8.

(76) Detre JA, Rao H, Wang DJ, Chen YF, Wang Z. Applications of arterial spin labeled MRI in the brain. J Magn Reson Imaging 2012 May;35(5):1026-37

(81) Westmark KD, Barkovich AJ, Sola A, Ferriero D, Partridge JC. Patterns and implications of MR contrast enhancement in perinatal asphyxia: a preliminary report. Ajnr: American Journal of Neuroradiology 1995 Apr;16(4):685-92.